京都大学学術情報リポジトリ
KURENAI 紅
Kyoto University Research Information Repository

京都大学
KYOTO UNIVERSITY

| | |
|---|---|
| Title | Inhibitory Mechanism for Amyloid β42 Aggregation by Catechol-type Flavonoids( Dissertation_全文 ) |
| Author(s) | Sato, Mizuho |
| Citation | Kyoto University (京都大学) |
| Issue Date | 2014-03-24 |
| URL | http://dx.doi.org/10.14989/doctor.k18328 |
| Right | 許諾条件により本文は2014-09-01に公開 |
| Type | Thesis or Dissertation |
| Textversion | ETD |

Kyoto University

# Inhibitory Mechanism for Amyloid $\beta$ 42 Aggregation by Catechol-type Flavonoids

Mizuho Sato

2014

# Inhibitory Mechanism for Amyloid β 42 Aggregation by Catechol-type Flavonoids

## Contents


| | | page |
|---|---|---|
| **Chapter 1** | General introduction | 1 |
| **Chapter 2** | Structure-activity relationship studies of (+)-taxifolin isolated from silymarin as an inhibitor of Aβ42 aggregation | 13 |
| **Chapter 3** | Inhibitory mechanism for Aβ42 aggregation by catechol-type flavonoids | 25 |
| **Chapter 4** | Solid-state NMR analysis of interaction sites between (+)-taxifolin and Aβ42 | 45 |
| **Summary and conclusion** | | 51 |
| **Acknowledgement** | | 53 |
| **References** | | 55 |
| **List of publications** | | 67 |

# Abbreviations

| | |
|---|---|
| Aβ | amyloid β protein |
| AD | Alzheimer's disease |
| APP | amyloid precursor protein |
| CD | circular dichroism |
| CP/MAS | cross polarization/magic angle spinning |
| DARR | dipolar-assisted rotational resonance |
| DIPEA | *N,N*-diisopropylethylamine |
| DMF | *N,N*-dimethylformamide |
| EGCG | (–)-epigallocatechin-3-gallate |
| EI-MS | electron ionization-mass spectrometry |
| Fmoc | 9-fluorenylmethyloxycarbonyl |
| HATU | 1-[bis(dimethylamino)methylene]-1*H*-1,2,3-triazolo[4,5-*b*] pyridinium 3-oxid hexafluorophosphate |
| HPLC | high performance liquid chromatography |
| $IC_{50}$ | half maximal (50%) inhibitory concentration |
| LC-MS | liquid chromatography-mass spectrometry |
| MALDI-TOF-MS | matrix-assisted laser desorption/ionization time-of-flight mass spectrometry |
| MTT | 3-(4,5-dimethylthiazol-2-yl)-2,5-diphenyltetrazolium bromide |
| NFTs | neurofibrillary tangles |
| Nle | norleucine |
| NMR | nuclear magnetic resonance |
| PBS | sodium phosphate-buffered saline |
| TCEP | tris(2-carboxyethyl)phosphine |
| TEM | transmission electron microscope |
| TFA | trifluoroacetic acid |
| Th-T | thioflavin-T |

# Chapter 1

# General introduction

*Alzheimer's disease*

Alzheimer's disease (AD) is the most common form of dementia. More than 36 million people have been diagnosed with dementia worldwide, with 60-80% of these having AD. The number of dementia patients is expected to increase to 115 million in 40 years.[1] One of the typical clinical presentations of AD is a progressive loss of memory and cognitive function, ultimately resulting in the loss of independence.

Two abnormal morphological changes in the cerebral cortex and hippocampus, senile plaques and neurofibrillary tangles (NFTs), are associated with AD. Senile plaques are deposits of amyloid β-protein (Aβ) that accumulate outside nerve cells, while NFTs are twisted fibers of hyperphosphorylated tau protein inside neuronal cells, and these morphological changes have been detected 25 years before the onset of symptoms. Bateman *et al.*.[2] recently reported the deposition of Aβ 15 years before the onset of symptoms, followed by brain amyloidosis, tau protein in the cerebrospinal fluid (CSF), hippocampal atrophy, and declines in cognitive and clinical functions (Fig. 1). Thus, Aβ, rather than tau protein, deposition occurs at the early stages in the pathogenesis of AD.

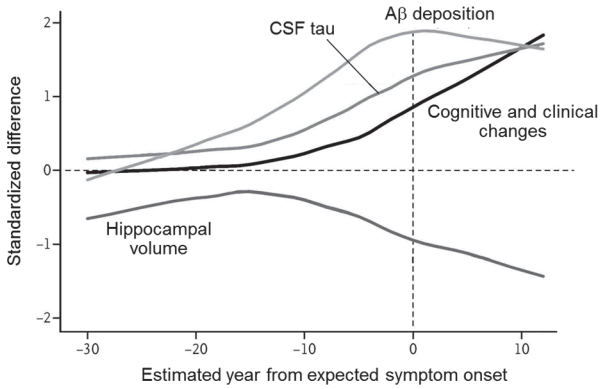


**Figure 1** Comparison of clinical, cognitive, and biochemical changes. Quoted from Ref. 2 with modifications. The vertical axis shows normalized differences between AD mutation carriers and non-carriers.

*Amyloid β-protein*

The amyloid cascade hypothesis plays a central role in the pathogenesis of AD.[3,4] This hypothesis proposes that Aβ aggregates form senile plaques and induce neuronal cell death. Aβ mainly consists of 40- and 42-mer proteins (Aβ40 and Aβ42)[5,6] that are generated from the amyloid protein precursor (APP) by β- and γ-secretases, respectively (amyloidogenic pathway, Fig. 2A). β-Secretase has been identified as an aspartyl protease of the pepsin family, called β-site APP-cleaving enzyme (BACE-1).[7] BACE-1 cleavage (β-cut) generates a membrane-bound APP C-terminal fragment (CTFβ), which is a precursor for the cleavage of γ-secretase (Fig. 2A). Two presenilin homologues, presenilin 1 (PS1) and presenilin 2 (PS2), have been shown to play an important role in the activity of γ-secretase. However, these presenilins require three other cofactors [nicastrin (Nct), anterior pharynx-defective phenotype (APH-1), and presenilin-enhancer (PEN-2)] to form a complex exhibiting γ-secretase activity.[7] The PS1 complex exhibits stronger activity than the PS2 complex. Other Aβ species (*e.g.* 37-, 38-, or 43-mer) are occasionally produced because the sites cleaved by γ-secretases at the C-terminal region of APP vary. The potent amyloidogenicity and pathogenicity of Aβ43 have been rediscovered.[8]

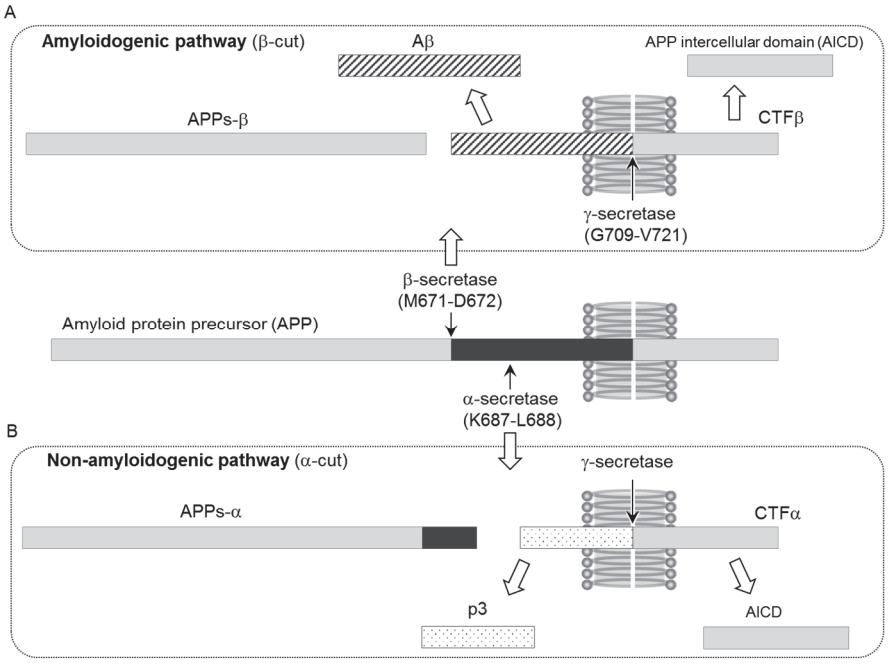


**Figure 2** APP processing by secretases.

In contrast, APP is cleaved by α-secretase between residues 16 and 17 to produce APPs-α and C83 (α-cut), and Aβ40 and Aβ42 are not generated from these cleaved precursors (non-amyloidogenic pathway, Fig. 2B). APP processing of α-secretase and γ-secretase produces a smaller fragment, referred to as p3 (N-terminal of CTFα) and APP intracellular domain (AICD). However, the physiological roles of these APP metabolites have yet to be elucidated in detail in spite of their ubiquitous expression in almost all human organs.[9)]

Although the ratio of Aβ40:Aβ42 is approximately 1:10 under physiological conditions, the aggregative ability and neurotoxicity of Aβ42 are higher than those of Aβ40. The ratio of Aβ40:Aβ42 has been shown to increase in patients with familial AD, the onset of which is 10~20 years earlier than sporadic AD, and approximately 24 mutations for APP and 199 mutations for presenilin have been identified to date.[10)] These findings suggest that Aβ42 plays a more pivotal role in the pathogenesis of AD.[4)] The mechanism of Aβ42 fibril formation can be explained by a nucleation-dependent polymerization model that consists of (1) a nucleation phase and (2) extension phase.[11,12)] In the nucleation phase, thermodynamically unstable nuclei serve as a rate-limiting step. Binding of monomers to such nuclei facilitates the formation of thermodynamically stable oligomers and fibrils.[13)]

*Amyloid oligomer hypothesis*

Insoluble Aβ fibrils had previously been considered to cause neuronal death.[14)] However, Walsh *et al*. demonstrated that the soluble Aβ oligomeric assembly, but not insoluble fibrils, was responsible for the pathology of AD, such as memory loss and neurodegeneration.[13,15,16)] Aβ oligomers are defined as soluble assemblies of Aβ that can induce synaptotoxicity and memory decline. Many types of Aβ oligomers have been identified, and at least two pathways of assembly[4,17)] have been shown to form insoluble protofibrils and fibrils ('on-pathway', Fig. 3) or high-molecular weight oligomers, such as Aβ*56 (12-mer), amylospheroids (150-700 kDa), and Aβ-derived diffusible ligands (ADDLs: ~90 kDa) ('off-pathway', Fig. 3), which are stable and do not form fibrils.[13)] These high-molecular weight oligomers cause synaptic dysfunction and excitotoxicity by blocking long-term potentiation (LTP) and facilitating

long-term depression (LTD), in spite of differences in their structure, stability, and concentration.[4] Furthermore, Aβ oligomers could accelerate the phosphorylation of the tau protein to reduce microtubule-binding capacity and form NFTs.[3]

Aβ oligomers have been shown to interact with membrane lipids and proteins.[18] Aβ is known to induce membrane-related toxicity by influencing the fluidity of the lipid bilayer, perturbing the structure and function of the plasma membrane, and promoting the release of lipids such as cholesterol from neuronal membranes, which disrupts neuronal lipid homeostasis. Furthermore, Aβ can bind to some membrane proteins; the Aβ monomer was shown to bind to the insulin receptor expressed in neurons and glial cells, thereby impairing the utilization of glucose, and Aβ assemblies interacted with *N*-methyl-D-aspartate (NMDA)-receptors, which are expressed in neurons, to induce internalization signals.[18]

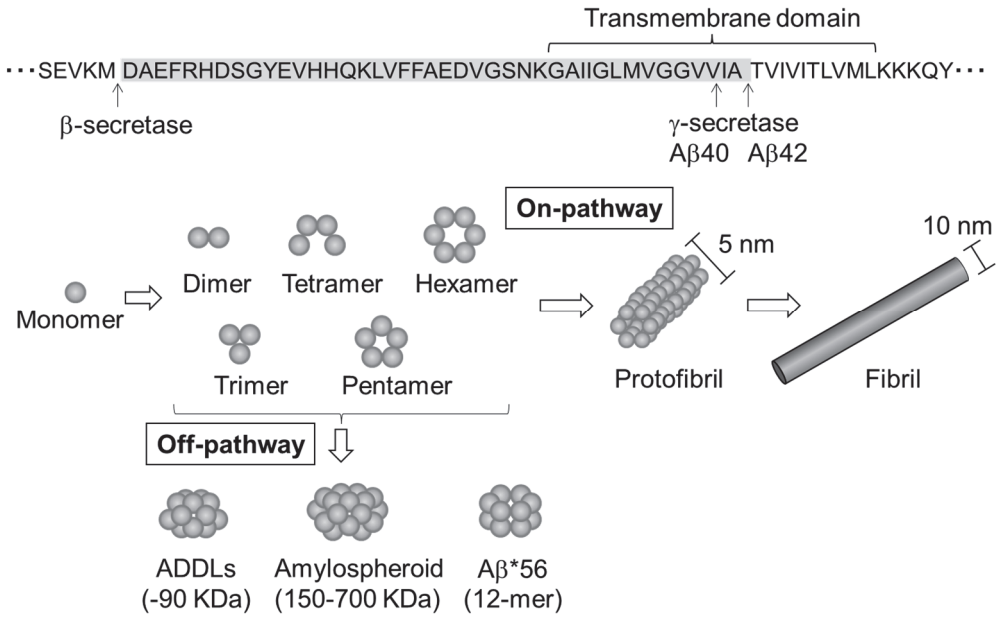


**Figure 3** Scheme of Aβ aggregation from oligomers to fibrils, showing both the 'on-pathway' and 'off-pathway'

*Oxidative stress via Aβ*

Oxidative stress is one of the major contributing factors to the progression of AD.[19] Extensive oxidative damage, including protein oxidation, lipid peroxidation, DNA damage, and mitochondrial dysfunction, has been reported in the AD brain (Fig. 4A).[20] Aβ-induced neurotoxicity has been shown to play a role in this oxidative damage through protein radicalization both *in vitro*[21,22] and *in vivo*.[23,24]

Transition metals, such as Cu(II), Zn(II), and Fe(III), are known to be enriched in senile plaques. Cu(II) has been shown to induce the radicalization of Aβ as well as generic proteins. The histidine residues at positions 6, 13, and 14, tyrosine residue at position 10 (Tyr10), and aspartic acid residues at positions 1 and 7 in Aβ are involved in the formation of a complex with Cu(II) (Fig. 4B, C).[25-27] Tyr10, in particular, is converted to a phenoxy radical through the reduction of Cu(II) to Cu(I), leading to the production of $H_2O_2$ (Fig. 4A).[28,29]

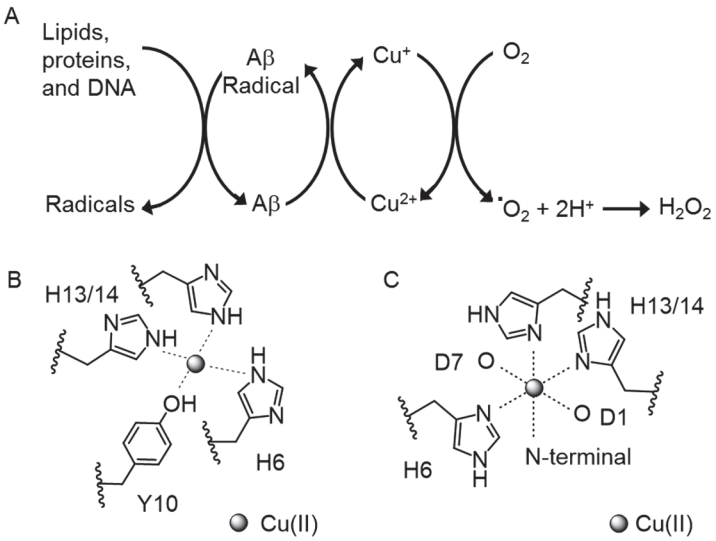


**Figure 4** (A) Cu(II) induces Aβ radicalization, which leads to the production of reactive oxygen species (ROS).[29] (B,C) The proposed binding model of Cu(II) with (B) His6,13,14 and Tyr10 in Aβ1-28[26] or (C) His13,14, Asp1,7 in Aβ42.[27] Quoted from Ref. 25 or 26 with modifications.

Met35 is another residue that plays a role in Aβ-induced neurotoxicity and oxidative stress.[21] The oxidative form (sulfoxide) of Met35 has been detected in the brains of AD patients.[30] This finding indicates that the *S*-oxidized radical cation can abstract an allylic hydrogen from the phospholipid acyl chain to generate allyl radicals, which is followed by the subsequent formation of lipid peroxides (Fig. 5A).[31] Pal *et al.*[32] reported that neurodegeneration is aggravated in knockout mice deficient in a methionine sulfoxide reductase isoform, suggesting the role of Met35 oxidation in the brain pathology of AD.

The *S*-oxidized radical cation is generally considered too unstable to cause continuous oxidative damage. Murakami *et al.*[22] recently reported the mechanism underlying Aβ42-induced neurotoxicity based on how the *S*-oxidized radical cation is stabilized for long-lasting oxidative stress. In this mechanism, the turn structure at Glu22 and Asp23 in Aβ42 moves the phenoxy radical at Tyr10 closer to Met35, generating *S*-oxidized radical cations (Fig. 5B). Moreover, another C-terminal turn at Gly38 and Val39 could enable the carboxylate anion at Ala42 to interact with the *S*-oxidized radical cation to form *S*-*O* bonding, which can stabilize the radical cation. The resultant hydrophobic core in the C-terminal region may accelerate Aβ aggregation concomitantly with this stabilization.

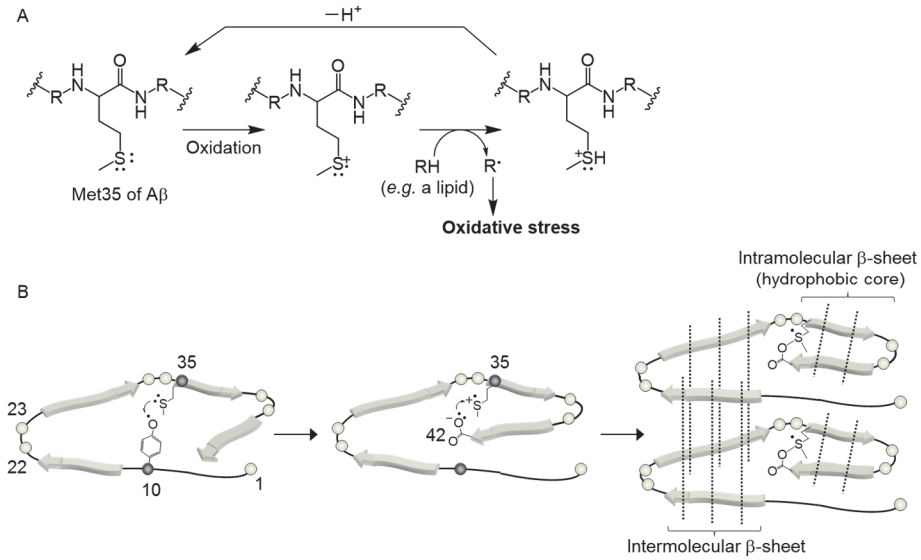


**Figure 5** (A) Methionine oxidation and subsequent radical formation. Quoted from Ref. 31 with modifications. (B) The mechanism of stabilization of *S*-oxidized radical cation in Met35.

*Therapeutic strategies targeting Aβ*

Several therapeutic agents against Aβ have been developed based on the amyloid oligomer hypothesis[33,34] to (1) decrease Aβ production, (2) inhibit Aβ aggregation, (3) enhance Aβ degradation, and (4) prevent the interaction between Aβ and the tau protein, and these have been referred to as disease-modifying agents (Fig. 6). On the other hand, symptom-alleviating agents are focused on improving neuronal function and protection. For example, the administration of acetylcholinesterase (AChE) and NMDA antagonists to improve cognitive function are widely accepted as the current standard treatment for AD worldwide. Although the AChE inhibitor, donepezil,[35] is available as a symptom-alleviating agent even in Japan, its effectiveness is limited and is not considered to be disease-modifying.[35-37]

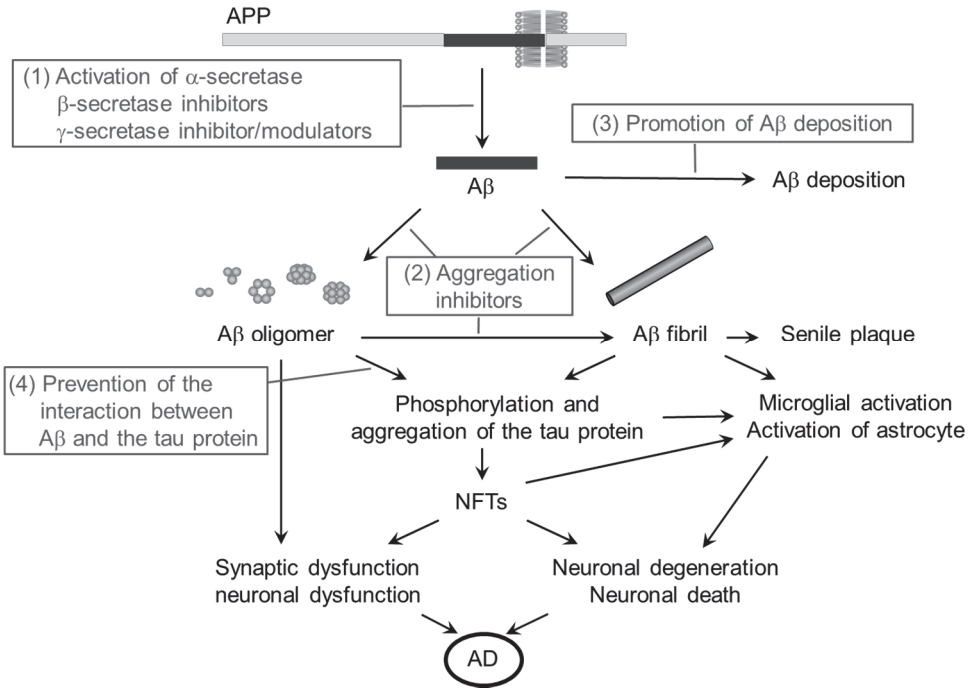


**Figure 6** Aβ-associated AD pathogenesis (black letters) and various therapeutic strategies (gray letters) composed of disease-modifying agents.

Several disease-modifying agents have been developed and advanced to clinical trials in recent years.[38] McLaurin *et al.*[39] demonstrated that *scyllo*-inositol (Fig. 7), an endogenous stereoisomer of inositol in humans, inhibited the aggregation of Aβ42 by preventing its transformation into β-sheets. Fibril formation and cytotoxicity in differentiated-PC12 cells were also prevented. The administration of *scyllo*-inositol to a transgenic mouse model of AD (TgCRND8 line) decreased plaque deposition, amount of amyloid in the brain, and synaptic dysfunction.[40] The presence of *scyllo*-inositol was also detected in the brain using gas chromatography-mass spectrometry.[41] *Scyllo*-inositol is currently undergoing clinical trials due to its favorable pharmacokinetics, safety, and tolerability (Phase II).

Synthetic inhibitors that limit Aβ42 aggregation have been reported. Because Lys residues play an important role in the assembly and toxicity of Aβ42 due to their hydrophobicity and the formation of electrostatic interactions, molecular tweezer CLR01 was designed to bind selectively to Lys residues in Aβ42 (Fig. 7).[42,43] CLR01 modified these properties of Lys residues by pinching the whole side chain of Lys and forming the salt bridge between the phosphonate of CLR01 and amino group of Lys residues. CLR01 was also shown to protect primary neurons from Aβ42-induced synaptotoxicity and ameliorate the accumulation of Aβ and the tau protein in a transgenic mouse model of AD (3xTg AD line).[44]

Metal ion-induced radical formation and aggregation are considered to be targets for anti-Aβ aggregation. PBT2, an 8-hydroxy quinolone (clioquinol, Fig. 7) analog, was designed based on the criteria of easier chemical synthesis, higher solubility, and blood-brain barrier permeability. PBT2 prevented the metal-induced aggregation of Aβ42 and generation of reactive oxygen species *in vitro*.[45] PBT2 was recently shown to reverse frontal lobe dysfunction and reduced Aβ42 levels in the CSF in a clinical trial (phase IIa).[46] PBT2 may inhibit radical formation of Aβ42 through the chelation of extracellular Cu(II) and Zn(II), resulting in the clearance of these ions.[45]

*Polyphenols as anti-Aβ42 aggregative agents*

AD is considered to be a lifestyle-related disease; therefore, the treatment or prevention of AD with dietary components has received a lot of attention.[12,47,48] Many studies have demonstrated the protective effects of various polyphenols derived from food products (*e.g.* turmeric, red wine, and green tea) against Aβ aggregation and neurotoxicity (Fig. 7).[49-51]

Curcumin is the main constituent of the spice turmeric, the daily intake of which has been attributed to the lower incidence of AD in India.[52,53] Curcumin exhibited a potent anti-amyloidogenic effect against Aβ *in vitro*, such as fibril formation, the destabilization of preformed fibrils, and oligomer formation *in vitro,*[54] and was also shown to preventively or therapeutically reduce amyloid plaques *in vivo.*[55] A previous study demonstrated that curcumin protected against Aβ-induced neurotoxicity in PC12 cells.[56] The binding of curcumin with Aβ is due to hydrophobicity (π-π stacking) deduced from the benzene ring.[57]

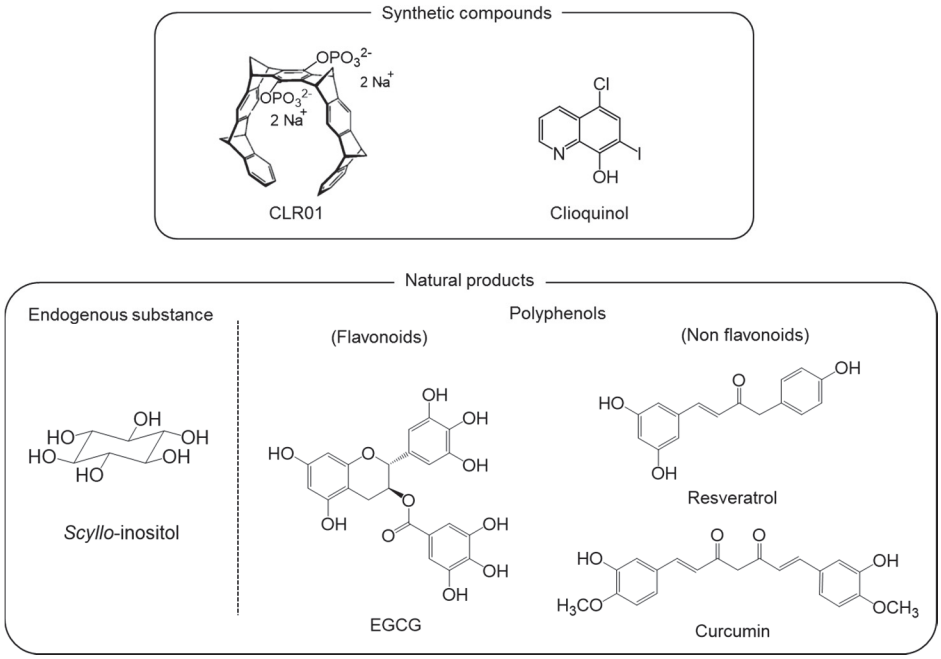


**Figure 7** Structures of Aβ42 aggregation inhibitors.

Epidemiological studies have suggested that the moderate consumption of red wine may protect against the development of AD.[58] Resveratrol, a component in red wine, prevented Aβ oligomer-induced neurotoxicity by remodeling toxic oligomers into non-toxic conformers.[59,60] It also lowered Aβ levels in AD model mice by promoting the non-amyloidogenic processing of APP through the enhanced activity of α-secretase.[61]

(–)-Epigallocatechin-3-gallate (EGCG), one of the main flavonoids in green tea, inhibited Aβ42 aggregation[49] by stabilizing Aβ42 as a non-toxic assembly.[62] Furthermore, EGCG protected hippocampal cells (primary cultured neurons from Sprague-Dawley rats) from Aβ-induced cell death,[63] and the *in vivo* administration of EGCG decreased Aβ levels and plaque formation by increasing the activity of α-secretase.[64]

Flavonoids are polyphenols that are commonly found in the human diet and plants. Many studies have examined the ability of flavonoids to reduce the production of Aβ production either by enhancing the activity of α-secretase or inhibiting that of β-secretase[51], to inhibit Aβ aggregation[49,65], and to enhance Aβ clearance[51].

Although curcumin, resveratrol, and EGCG are currently undergoing clinical or preclinical trials for the treatment of AD, most trials have reported conflicting results.[47,66] No significant difference was observed in Mini-Mental State Examination (MMSE; the most commonly used test for complaints of memory problems) scores or in Aβ plasma levels in patients treated with 1 or 3 g curcumin per day for 6 months.[67] Clinical trials using resveratrol and EGCG are currently being conducted. The above findings for curcumin motivated us to verify the interaction between polyphenols and Aβ so that polyphenols could be developed as therapeutic agents for AD. Regarding the molecular interaction between Aβ and flavonoids, a docking simulation by Keshet *et al.*[68] predicted the involvement of Lys28 and the C-terminal region in the binding with myricetin. However, the precise mode of binding with flavonoids has not been elucidated in detail, except for limited studies using NMR spectroscopy [curcumin[69], EGCG[70,71], and myricetin[72]].

*Objectives*

Silymarin, a seed extract of *Silybum marianum* that contains flavonolignane diastereomers,[73] has been used as an anti-hepatotoxic medicine without notable adverse effects,[74] and is particularly efficacious against the damage induced by alcohol and disturbances in the function of the gastrointestinal tract.[75] Murata *et al.*[76] recently demonstrated that silymarin attenuated AD-like pathological features, such as senile plaques, neuronal inflammation, behavioral dysfunction, and Aβ oligomer formation in a well-established AD mouse model (J20 line).

The purpose of this study is to clarify the inhibitory mechanism for Aβ42 aggregation by polyphenols. Concretely speaking, (+)-taxifolin was identified as one of the active components among six flavonoids isolated from silymarin. Structure-activity relationship studies were performed using methylated (+)-taxifolin and taxifolin enantiomers to clarify the structure of (+)-taxifolin required for the anti-aggregative properties of Aβ42 (Chapter 2). In Chapter 3, the involvement of autoxidation in the inhibitory ability of (+)-taxifolin against Aβ42 aggregation in the presence of an oxidant or under anaerobic conditions was estimated using Th-T, UV spectrometry, and CD spectrometry. Based on these results, together with other catechol-type flavonoids, an inhibitory mechanism was proposed for Aβ42 aggregation by catechol-type flavonoids. The mechanisms by which (+)-taxifolin as a catechol-type polyphenol and curcumin as a non-catechol-type one interacted with the β-sheet region through π/π stacking and hydrophobicity were compared using solid-state NMR experiments (Chapter 4).

# Chapter 2

# Structure-activity relationship studies of (+)-taxifolin isolated from silymarin as an inhibitor of Aβ42 aggregation*

## Introduction

As mentioned in Chapter 1, Murata *et al.*[76] reported that silymarin suppressed the aggregation and the neurotoxicity in PC12 cells of Aβ42 *in vitro*, and then they treated J20 mice with a powdered diet containing 0.1% silymarin for 6 months. Silymarin rescued senile plaques and the amount of Aβ oligomers in the mouse brain as well as the behavioral dysfunction, but almost no significant changes in BACE-1 activity was observed. These results suggest that the protective effect of silymarin on Aβ accumulation could be originated from the inhibition of Aβ aggregation, rather than the attenuation of Aβ production. Although silymarin is known as a mixture of flavonolignan diastereomers,[73] such as silibinin, silydianin, and silychristin, the effect of these components on Aβ42 aggregation has not yet been examined.

In this Chapter, the author screened the compounds focusing on the flavonoids from silymarin with an anti-aggregative ability against Aβ42, and then examined the structure-activity relationships of the compound to investigate its essential moiety required for the inhibition of Aβ42 aggregation.

---

*The content described in this Chapter was originally published in *Bioscience, Biotechnology and Biochemistry*. Mizuho Sato, Kazuma Murakami, Mayumi Uno, Haruko Ikubo, Yu Nakagawa, Sumie Katayama, Ken-ichi Akagi and Kazuhiro Irie: Structure-activity relationship for (+)-taxifolin isolated from silymarin as an inhibitor of amyloid β aggregation. *Biosci. Biotechnol. Biochem.* 2013; *77*: 1100-1103 © The Japan Society for Bioscience, Biotechnology, and Agrochemistry.

## Results

*Isolation of (+)-taxifolin as an active component in silymarin*

Silymarin was fractionated by column chromatography followed by high performance liquid chromatography (HPLC) to yield six kind of flavonoids; silibinin A (isolated yield 6.7%),[77] silibinin B (isolated yield 10%),[77] silydianin (isolated yield 8.4%),[78] (+)-taxifolin (isolated yield 2.2%),[79] isosilychristin (isolated yield 1.3%),[80] and silychristin (isolated yield 8.4%)[81] (Fig. 8A). Effects of these flavonoids on Aβ42 aggregation were examined using the assay of thioflavin-T (Th-T), a regent that fluoresces when bound to Aβ aggregates, and using transmission electron microscopy (TEM), as previously described.[82,83] Only (+)-taxifolin, a catechol-type flavonoid, among the isolated flavonoids significantly reduced the Th-T fluorescence induced by Aβ42, meaning the potent inhibition of Aβ42 aggregation by (+)-taxifolin (Fig. 8B). In the analysis of TEM, Aβ42 formed the typical fibril, but shorter or slighter fibrils were observed in the case of Aβ42 incubated with (+)-taxifolin (Fig. 9C). These inhibitory effects of (+)-taxifolin on Aβ42 aggregation were almost equal to that of silymarin, indicating the (+)-taxifolin as one of the active components (Fig. 8B). Moreover, (+)-taxifolin disaggregated the preformed fibrils of Aβ42 (Fig. 8C).

To test the effect on the neurotoxicity of Aβ42, the author carried out the MTT assay using PC12 cells, which are sensitive to Aβ peptide and are generally used for detecting cytotoxicity as a neurotoxicity model.[84] (+)-Taxifolin was neuroprotective in a dose-dependent manner (Fig. 8D).

*Structure-activity relationship of (+)-taxifolin for anti-Aβ42 aggregation*

To identify which hydroxyl groups of (+)-taxifolin are involved in the inhibitory effect, four *O*-methyl derivatives of (+)-taxifolin were prepared by diazomethane treatment (Scheme 1A). In the Th-T assay, (+)-7-*O*-methyl-taxifolin prevented the aggregation of Aβ42 in a manner similar to (+)-taxifolin, whereas (+)-7,3'-di-*O*-methyl-, (+)-7,4'-di-*O*-methyl-, and (+)-7,3',4'-tri-*O*-methyltaxifolin did not (Fig. 9A). In TEM images, Aβ42 fibrils treated with (+)-7-*O*-methyl-taxifolin, but not with (+)-7,3'-di-*O*-methyl-taxifolin, were similar to those treated with (+)-taxifolin (Fig. 9C). These results indicate 3',4'-dihydroxyl groups (catechol structure)

on the B-ring of (+)-taxifolin to be important to prevent Aβ42 aggregation, whereas the 7-hydroxyl group is less.

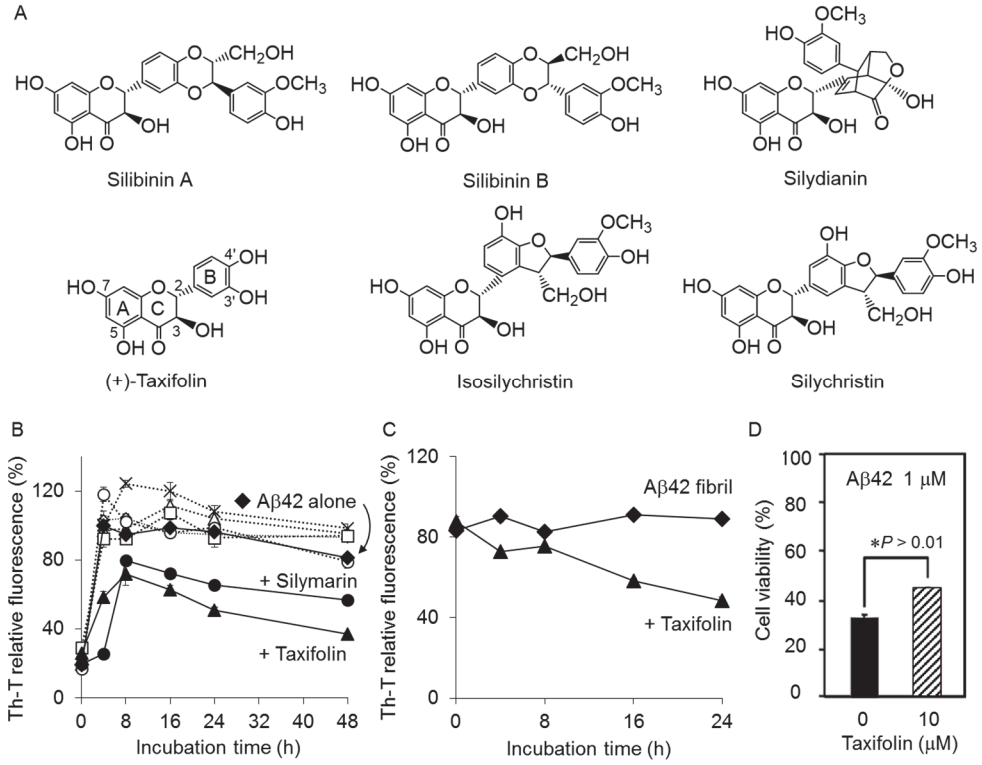


**Figure 8** (A) Structure of the flavonoids isolated from silymarin. (B) The effect of each flavonoid on Aβ42 aggregation was estimated by the Th-T method. Aβ42 (25 μM) was incubated with or without each flavonoid (50 μM) in PBS (50 mM sodium phosphate, 100 mM NaCl, pH 7.4) at 37 °C. ◆, Aβ42 without flavonoid; ▲, Aβ42 with (+)-taxifolin; ●, Aβ42 with silymarin; ◇, Aβ42 with silibinin A; △, Aβ42 with silibinin B; □, Aβ42 with silydianin; ○, Aβ42 with isosilychristin and ×, Aβ42 with silychristin. The molecular weight of silymarin was defined as 482, which was that of the main components (silibinin A and B, silydianin, isosilychristin, and silychristin) in silymarin. Data are presented as the mean ± s.e.m. ($n$ = 8). (C) The effect of (+)-taxifolin on the preformed fibrils of Aβ42. ◆, Aβ42 fibril (56.4 μg/500 μL) without flavonoid and ▲, Aβ42 fibril (56.4 μg/500 μL) with (+)-taxifolin (50 μM); (D) The effect of (+)-taxifolin on Aβ42-induced neurotoxicity on PC12 cells using MTT assay.

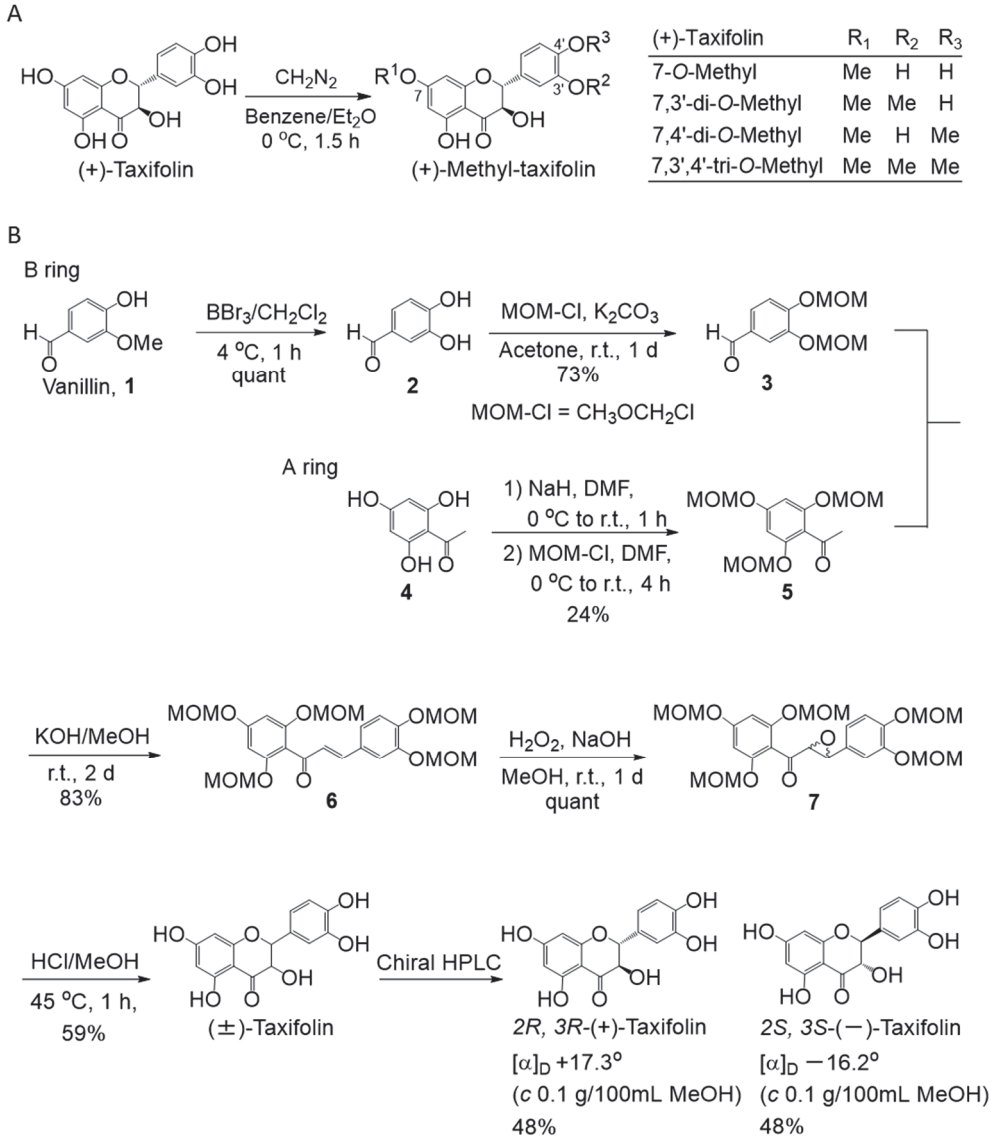


**Scheme 1** (A) Methylation of (+)-taxifolin. (B) Synthesis (+)- and (–)-taxifolin synthesis by the route of Roschek *et al.*[85)]

(+)-Taxifolin was not methylated at position 5 on the A-ring by diazomethane, implying that the hydroxyl group at position 5 could not be involved in the intermolecular interaction. Indeed, the hydroxyl group at position 5 of (+)-taxifolin could participate in the intramolecular hydrogen bond with the carbonyl oxygen on the C-ring, which was deduced from the $^{1}$H NMR chemical shift [11.7 ppm in $(CD_3)_2CO$]. The practical implication

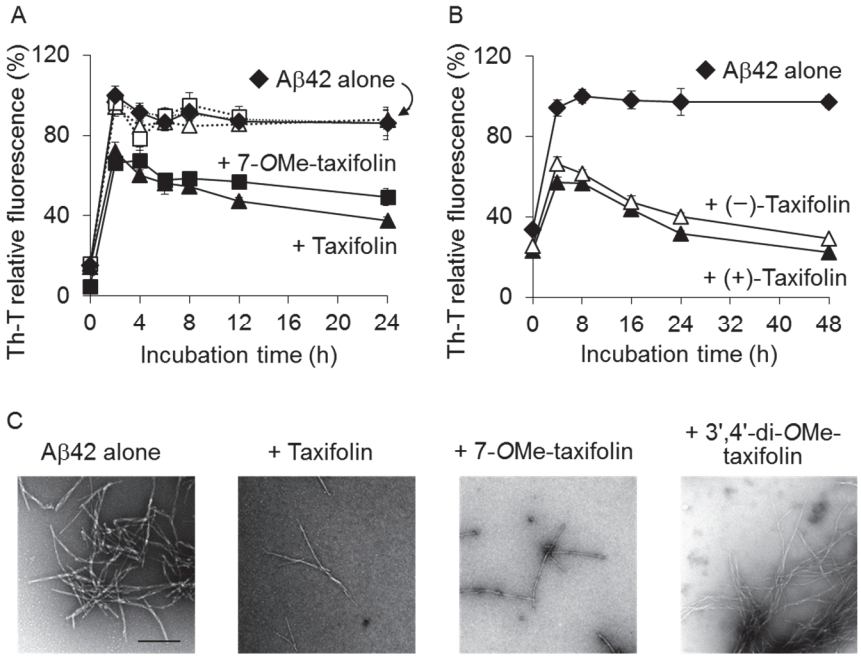


**Figure 9** (A) The inhibitory effects of methylated (+)-taxifolins on Aβ42 aggregation determined by the Th-T assay. Aβ42 (25 μM) was incubated with or without each flavonoid (50 μM) in PBS at 37 °C. ◆, Aβ42 without flavonoid; ▲, Aβ42 with (+)-taxifolin; ■, Aβ42 with (+)-7-*O*-methyl-taxifolin; ◇, Aβ42 with (+)-7,3'-di-*O*-methyl-taxifolin; △, Aβ42 with (+)-7,4'-di-*O*-methyl-taxifolin and □, Aβ42 with (+)-7,3',4'-tri-*O*-methyl-taxifolin. Data are presented as the mean ± s.e.m. ($n$ = 8). (B) The effects of the stereochemistry on the C-ring in (+)-taxifolin on Aβ42 aggregation were evaluated by the Th-T test. ◆, Aβ42 (25 μM) without flavonoid; ▲, Aβ42 (25 μM) with (+)-taxifolin and △, Aβ42 with (–)-taxifolin (50 μM). (C) The TEM analysis of Aβ42 fibrils treated with the (+)-taxifolin derivatives. Aβ42 (25 μM) was incubated with or without each flavonoid (50 μM) in PBS at 37 °C for 48 h. Scale bar, 200 nm.

of this result is that the hydroxyl group at position 5 does not contribute to the inhibition of Aβ42 aggregation by (+)-taxifolin. Although the methylated (+)-taxifolin at position 3 on the C-ring was not also obtained, the report[86] that luteolin without a hydroxyl group at position 3 inhibited Aβ42 aggregation means that the hydroxyl group at position 3 of (+)-taxifolin would not participate in the inhibitory activity.

Finally, (–)-taxifolin, 2,3-(*S,S*)-*trans* form, was synthesized to examine the effect of the stereochemistry at position 2 and 3 on the C-ring of (+)-taxifolin, 2,3-(*R,R*)-*trans* form, on the inhibition of Aβ42 aggregation (Scheme 1B). The inhibitory ability against Aβ42 aggregation was almost the same between these two enantiomers. Regarding the slight difference of the inhibition of Aβ42 aggregation by (+)-taxifolin between Figs. 8 and 9, the fluorescence intensity in the Th-T assay are sometimes influenced by several factors, for example, outside temperature, batch of Aβ42, and so on. However, similar results were obtained by another independent experiment.

Several groups reported no difference of the inhibitory activities against Aβ40 or Aβ42 aggregation between (+)-catechin (2,3-*trans* form, Fig. 10) and (–)-epicatechin (2,3-*cis* form, Fig. 10).[87] Furthermore, myricetin and quercetin (Fig. 10) with a double bond between C2 and C3 on the C-ring were previously reported to inhibit Aβ42 aggregation.[12] These findings did not contradict the results obtained in Fig. 9B; the stereochemistry at positions 2 and 3 not to play an important role in the inhibitory effects of (+)-taxifolin against Aβ42 aggregation.

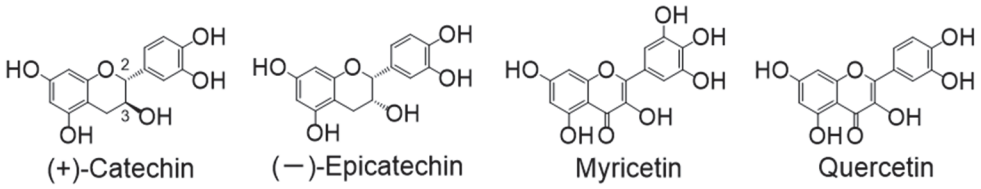


**Figure 10** Structure of flavonoids having inhibitory ability of Aβ aggregation.

## Discussion

There were some reports on the preventive role of silymarin in the inflammation and grail activation by inhibiting the production of inflammatory factors such as NF-κB, TNF-α, iNOS and COX-2, leading to neuroprotection.[88] The anti-neuroinflammation by silymarin observed in the previous studies[76] might be associated with these benefits by silymarin. We identified (+)-taxifolin as one of the active components with anti-aggregative ability against Aβ42 from silymarin, and this is the first report that (+)-taxifolin has a preventive effect on Aβ42 aggregation. The quantification analysis using HPLC revealed that silymarin contained 1.2% (+)-taxifolin, which was slightly less than the isolated yield (2.2%, purity 99.6%). The low content rate of (+)-taxifolin does not exclude the existence of other active components in silymarin.

The structure-activity relationship studies of (+)-taxifolin clarified the requisite moiety (catechol structure on B-ring) for inhibitory activity against Aβ42 aggregation, which is consistent with the findings that only (+)-taxifolin has a catechol moiety among the flavonoids isolated from silymarin in this study. These findings do not contradict the report by Akaishi *et al.*[86] that the 3',4'-dihydroxyl group, not the 7-hydroxyl group, is essential to the inhibitory effect of fisetin (quercetin analog without 5-hydroxyl group) on Aβ42 fibril formation. A detailed inhibitory mechanism for Aβ42 aggregation by such a catechol-type flavonoid will be discussed in the following Chapters.

## Experimental procedure

*General remarks*

The following spectroscopic and analytical instruments were used: $^1$H NMR, AVANCE III 500 and AVANCE III 400 (Bruker, Germany); EI-MS, JMS-600H (70 eV, 300 μA; JEOL, Tokyo, Japan); polarimeter, P-2200 (Jasco, Tokyo, Japan); matrix-assisted laser desorption/ionization time-of-flight mass spectrometry (MALDI-TOF-MS), AXIMA-CFR (Shimadzu, Kyoto, Japan); high performance liquid chromatography (HPLC), Waters 600E multisolvent delivery system with 2487 UV dual λ absorbance detector (Milford, MA); transmission electron microscopy (TEM), H-7650 electron microscope (Hitachi, Ibaraki, Japan); micro-plate reader, MPR-A4ιII, (TOSOH, Tokyo, Japan), or Fluoroskan Ascent (Thermo Scientific, Rockford, IL); peptide synthesizer, Pioneer™ peptide synthesizer (Applied Biosystems, Foster City, CA).

Following *N*-α-(9-fluorenylmethoxycarbonyl) (Fmoc) amino acid were used for peptide synthesis: Ala-OH, Asn(Trt)-OH, Asp(O*t*Bu)-OH, Arg(Pbf)-OH, Gln(Trt)-OH, Glu(O*t*Bu)-OH, Gly-OH, His(Trt)-OH, Ile-OH, Leu-OH, Lys(Boc)-OH, Met-OH, Phe-OH, Ser(*t*Bu)-OH, Tyr(*t*Bu)-OH, Val-OH (Applied Biosystems). 1-[bis(dimethylamino)methylene]-1*H*-1,2,3-triazolo[4,5-*b*] pyridinium 3-oxid hexafluorophosphate (HATU), Fmoc-L-Ala-polyethylene glycol-polystylene support (PEG-PS) resin, and *N,N*-diisopropylethylamine (DIPEA) were purchased from Applied biosystems. *N,N*-Dimethylformamide (DMF), trifluoroacetic acid (TFA), 1,2-ethanedithiol, thioanisole, *m*-cresol, and diethyl ether (peroxide free) were obtained from Nacalai tesque (Kyoto, Japan).

*Separation of silymarin*

Silymarin (lot no. 228-216, LKT Laboratories, St. Paul, MN) was fractionated by column chromatography eluted with 5.0% MeOH/$CHCl_3$ on Wakogel C-200 (Wako, Osaka, Japan) to give two major fractions containing flavonoids. The first fraction was chromatographed by HPLC on a YMC-Pack ODS-A column (20 mm i.d. x 150 mm; YMC, Kyoto, Japan) using 50% MeOH/$H_2O$ to yield silibinin A (16 mg from 240 mg of silymarin)[77)] and silibinin B (25 mg from 240 mg of silymarin),[77)] and using 40% MeOH/$H_2O$ to yield silydianin (31 mg from 370 mg of silymarin),[78)] respectively. The second fraction was separated on a YMC-Pack ODS-AL column (20 mm i.d. x 150 mm; YMC) using 40% MeOH/$H_2O$ to give (+)-taxifolin (6.7 mg from 310 mg of silymarin),[79)] isosilychristin (3.9 mg from 310 mg of silymarin),[80)] and silychristin (26 mg from 310 mg of silymarin)[81)] (Fig. 8A). The structures of these compounds were confirmed by $^1$H NMR[77-81)], EI-MS, and specific optical rotation (P-2200).

Silibinin A: $^1$H NMR (500 MHz, 295.0 K, acetone-$d_6$, 31.9 mM, ref. tetramethylsilane) δ 3.52 (1H, dd, $J$ = 12.4, 4.3 Hz), 3.75 (1H, dd, $J$ = 12.4, 2.5 Hz), 3.87 (3H, s), 4.16 (1H, ddd, $J$ = 7.0, 4.3, 2.5 Hz), 4.64 (1H, d, $J$ = 11.5 Hz), 5.00 (1H, d, $J$ = 8.0 Hz), 5.07 (1H, d, $J$ = 11.5 Hz), 5.94 (1H, d, $J$ = 2.1 Hz), 5.97 (1H, d, $J$ = 2.1 Hz), 6.89 (1H, d, $J$ = 8.1 Hz), 6.96 (1H, d, $J$ = 8.3 Hz), 6.99 (1H, dd, $J$ = 8.1, 1.9

Hz), 7.09 (1H, dd, $J$ = 8.3, 2.0 Hz), 7.15 (1H, d, $J$ = 1.9 Hz), 7.16 (1H, d, $J$ = 2.0 Hz). EI-MS: *m/z*, calcd: 482, found: 482 $[M]^+$). $[\alpha]_D$ +26.0° (*c* 0.25, MeOH, 25.6 °C).

Silibinin B: $^1$H NMR (500 MHz, 295.0 K, acetone-$d_6$, 26.9 mM, ref. tetramethylsilane) δ 3.52 (1H, dd, $J$ = 12.4, 4.2 Hz), 3.75 (1H, dd, $J$ = 12.4, 2.5 Hz), 3.88 (3H, s), 4.15 (1H, ddd, $J$ = 8.0, 4.2, 2.5 Hz), 4.65 (1H, d, $J$ = 11.5 Hz), 5.00 (1H, d, $J$ = 8.0 Hz), 5.09 (1H, d, $J$ = 11.5 Hz), 5.96 (1H, d, $J$ = 2.0 Hz), 5.99 (1H, d, $J$ = 2.0 Hz), 6.88 (1H, d, $J$ = 8.1 Hz), 6.97 (1H, d, $J$ = 8.3 Hz), 6.99 (1H, dd, $J$ = 8.1, 1.9 Hz), 7.10 (1H, dd, $J$ = 8.3, 2.0 Hz), 7.15 (2H, t, $J$ = 2.0 Hz). EI-MS: *m/z*, calcd: 482, found: 482 $[M]^+$). $[\alpha]_D$ +12.0° (*c* 0.19, MeOH, 25.9 °C).

Silydianin: $^1$H NMR (500 MHz, 295.0 K, acetone-$d_6$, 41.5 mM, ref. tetramethylsilane) δ 2.93 (1H, brs), 3.28 (1H, dd, $J$ = 6.8, 2.9 Hz), 3.41 (1H, brs), 3.67 (1H, dd, $J$ = 4.1, 2.1 Hz), 3.88 (1H, d, $J$ = 7.8 Hz), 4.29 (1H, dd, $J$ = 7.8, 3.2 Hz), 4.65 (1H, d, $J$ = 11.3 Hz), 4.92 (1H, d, $J$ = 11.3 Hz), 6.00 (2H, s), 6.20 (1H, dd, $J$ = 6.9, 1.4 Hz), 6.76 (2H, s), 6.89 (1H, s). EI-MS: *m/z*, calcd: 482, found: 482 $[M]^+$). $[\alpha]_D$ +230° (*c* 0.005, MeOH, 26.8 °C).

(+)-Taxifolin: $^1$H NMR (400 MHz, 296.9 K, acetone-$d_6$, 3.94 mM, ref. tetramethylsilane) δ4.58 (1H, d, $J$ = 11.5 Hz), 4.99 (1H, d, $J$ = 11.5 Hz), 5.92 (1H, d, $J$ = 2.1 Hz), 5.96 (1H, d, $J$ = 2.1 Hz), 6.84 (1H, d, $J$ = 8.1 Hz), 6.90 (1H, dd, $J$ = 8.1, 1.9 Hz), 7.05 (1H, d, $J$ = 1.9 Hz), 11.7 (1H, brs). EI-MS: *m/z*, calcd: 304, found: 304 $[M]^+$). $[\alpha]_D$ +22.2° (*c* 0.12, MeOH, 29.1 °C).

Silychristin: $^1$H NMR (500 MHz, 295.0 K, acetone-$d_6$, 41.5 mM, ref. tetramethylsilane) δ 3.61 (1H, ddd, $J$ = 6.9, 6.8, 5.5 Hz), 3.84 (3H, s), 3.86 (1H, dd, $J$ = 10.8, 6.8 Hz), 3.92 (1H, dd, $J$ = 10.8, 5.5 Hz), 4.63 (1H, d, $J$ = 11.6 Hz), 5.04 (1H, d, $J$ = 11.6 Hz), 5.58 (1H, d, $J$ = 6.9 Hz), 5.95 (1H, d, $J$ = 2.0 Hz), 5.99 (1H, d, $J$ = 2.0 Hz), 6.83 (d, 1H, $J$ = 8.1 Hz), 6.93 (1H, dd, $J$ = 8.1, 1.9 Hz), 6.99 (1H, brd, $J$ = 1.1 Hz), 7.02 (1H, brs), 7.10 (1H, d, $J$ = 1.9 Hz). EI-MS: *m/z*, calcd: 482, found: 482 $[M]^+$). $[\alpha]_D$ +112° (*c* 0.30, MeOH, 26.3 °C).

Isosilychristin: $^1$H NMR (500 MHz, 295.0 K, acetone-$d_6$, 7.05 mM, ref. tetramethylsilane) δ 3.66 (1H, dd, $J$ = 10.8, 8.9 Hz), 3.76 (3H, s), 3.86 (1H, ddd, $J$ = 8.8, 4.5, 3.0 Hz) 3.96 (1H, dd, $J$ = 10.8, 4.5 Hz), 4.64 (1H, d, $J$ = 11.7 Hz), 5.24 (1H, d, $J$ = 11.7 Hz), 5.68 (1H, d, $J$ = 3.0 Hz), 5.90 (1H, d, $J$ = 2.1 Hz), 5.93 (1H, d, $J$ = 2.1 Hz), 6.75 (1H, d, $J$ = 8.1 Hz), 6.84 (1H, d, $J$ = 8.4 Hz), 6.89 (1H, dd, $J$ = 8.1, 2.0 Hz), 6.99 (1H, d, $J$ = 2.0 Hz), 7.08 (2H, d, $J$ = 8.4 Hz). EI-MS: *m/z*, calcd: 482, found: 482 $[M]^+$). $[\alpha]_D$ +206° (*c* 0.005, MeOH, 26.4 °C).

*Methylation of (+)-taxifolin*

*N*-Methyl–*N*-nitroso-*p*-toluenesulfonamide dissolved in ether/EtOH (35 mL/15 mL, 0.20 mM) was heated at 70 °C. To the solution was added a potassium hydroxide solution (one gram of potassium hydroxide in 15 mL of water) to yield diazomethane, which was condensed in a cold tube as a yellow ether solution. (+)-Taxifolin (65 mg, 0.21 mmol) was dispersed in benzene (1.0 mL) and diethylether (3.0 mL), to which an aliquot of the diazomethane solution (12 mL) was added at 0 °C, and the mixture was stood at the same temperature for 1.5 h. The solution was evaporated *in vacuo*, and the residue was separated by preparative thin layer chromatography, followed by HPLC on a YMC-Pack ODS-A column (20 mm

i.d. x 150 mm; YMC) with a linear gradient of 50-100% $CH_3CN/H_2O$ for 30 min to yield (+)-7-*O*-methyl- (18 mg, 28% yield), (+)-7,3'-di-*O*-methyl- (6.3 mg, 9.7% yield), (+)-7,4'-di-*O*-methyl- (7.3 mg, 11% yield), and (+)-7,3',4'-tri-*O*-methyl-taxifolin (2.1 mg, 3.2% yield, Scheme 1A). Their structures were confirmed by $^1$H NMR[79] and EI-MS to be identical to those reported previously.

(+)-7-*O*-Methyl-taxifolin: $^1$H NMR (400 MHz, 296.8 K, acetone-$d_6$, 16.3 mM, ref. tetramethylsilane) δ 3.85 (3H, s), 4.64 (1H, d, $J$ = 11.5 Hz), 5.04 (1H, d, $J$ = 11.4 Hz), 6.04 (1H, d, $J$ = 2.2 Hz), 6.07 (1H, d, $J$ = 2.3 Hz), 6.85 (1H, d, $J$ = 8.1 Hz), 6.90 (1H, d, $J$ = 8.0 Hz), 7.05 (1H, brs). EI-MS: *m/z*, calcd: 318, found: 318 $[M]^+$.

(+)-7,3'-*O*-Methyl-taxifolin: $^1$H-NMR (400 MHz, 296.8 K, acetone-$d_6$, 16.3 mM, ref. tetramethylsilane) δ 3.85 (3H, s), 3.87 (3H, s), 4.72 (1H, d, $J$ = 11.8 Hz), 5.10 (1H, d, $J$ = 11.8 Hz), 6.04 (1H, d, $J$ = 2.3 Hz), 6.07 (1H, d, $J$ = 2.3 Hz), 6.86 (1H, d, $J$ = 8.1 Hz), 7.03 (1H, dd, $J$ = 8.2 , 2.0 Hz), 7.21 (1H, d, $J$ = 2.0 Hz). EI-MS: *m/z*, calcd: 332, found: 332 $[M]^+$.

(+)-7,4'-*O*-Methyl-taxifolin: $^1$H NMR (400 MHz, 296.8 K, acetone-$d_6$, 9.94 mM, ref. tetramethylsilane) δ 3.85 (3H, s), 3.87 (3H, s), 4.66 (1H, dd, $J$ = 11.5, 3.1 Hz) , 4.75 (1H, brd, $J$ = 3.7 Hz), 5.09 (1H, d, $J$ = 11.5 Hz), 6.05 (1H, d, $J$ = 2.2 Hz), 6.07 (1H, d, $J$ = 2.2 Hz), 6.97 (1H, d, $J$ = 8.2 Hz), 7.00 (1H, dd, $J$ = 8.3, 1.8 Hz), 7.08 (1H, d, $J$ = 1.9 Hz). EI-MS: *m/z*, calcd: 332, found: 332 $[M]^+$.

(+)-7,3',4'-*O*-Methyl-taxifolin: $^1$H NMR (400 MHz, 296.8 K, acetone-$d_6$, 4.04 mM, ref. tetramethylsilane) δ 3.83 (3H, s), 3.84 (3H, s), 3.86 (3H, s), 4.73-4.76 (1H, m), 5.13 (1H, d, $J$ = 11.1 Hz), 6.05 (1H, d, $J$ = 2.2 Hz), 6.08 (1H, d, $J$ = 2.2 Hz), 6.98 (1H, d, $J$ = 8.3 Hz), 7.10 (1H, dd, $J$ = 8.3, 2.0 Hz), 7.22 (1H, d, $J$ = 2.0 Hz). EI-MS: *m/z*, calcd: 346, found: 346 $[M]^+$.

*Synthesis of (–)-taxifolin*

(–)-Taxifolin, 2,3-(*S,S*)-*trans* form, was synthesized basically according to the method of Roschek *et al.,*[85] except for the use of 3,4-trihydroxybenzaldehyde as a substrate. Briefly, vanillin (0.10 g, 0.63 mmol) dissolved in $CH_2Cl_2$ was demethylated by treatment with 1 M boron tribromide in dichloromethane (2.6 mL, 2.6 mmol) at 4 $^oC$ for 1 h to give quantitatively 3,4-dihydroxybenzaldehyde. The phenolic hydroxyl groups were protected with methoxymethyl groups (73% yield). On the other hand, the phenolic hydroxyl groups of 2,4,6-trihydroxyacetophenone were also protected with methoxymethyl groups (24% yield). A cross-aldol reaction of these two products in KOH/MeOH (83% yield), followed by treatment with $H_2O_2$ under alkaline condition, yielding quantitatively the epoxide, which was cyclized and deprotected under HCl/MeOH to give (±)-taxifolin (59% yield). Enantiomers were separated by HPLC on a CHIRALCEL OJ-RH column (10 mm i.d. x 150 mm; Daicel Corporation, Osaka, Japan) using 15% $CH_3CN/H_2O$ containing 0.1% acetic acid.[89] The ratio of enantiomers was almost 1 : 1, based on the isolated yield of each enantiomer:

(+)-taxifolin: $^1$H NMR (400 MHz, 297.1 K, acetone-$d_6$, 19.7 mM, ref. tetramethylsilane) δ 4.60 (1H, d, $J$ = 11.6 Hz), 5.01 (1H, d, $J$ = 11.6 Hz), 5.94 (1H, d, $J$ = 2.0 Hz), 5.98 (1H, d, $J$ = 2.0 Hz), 6.85 (1H, d, $J$ = 8.0 Hz), 6.91 (1H, dd, $J$ = 8.0,

2.0 Hz), 7.06 (1H, d, $J$ = 2.0 Hz). $[\alpha]_D$ +17.3° ($c$ 0.10, MeOH, 16 °C, lit.[80] $[\alpha]_D$ +19.0°, $c$ 0.1, MeOH).

(–)-taxifolin: $^1$H NMR (400 MHz, 297.1 K, acetone-$d_6$, 19.7 mM, ref. tetramethylsilane) δ 4.61 (1H, d, $J$ = 11.2 Hz), 5.02 (1H, d, $J$ = 11.6 Hz), 5.95 (1H, s), 5.98 (1H, s), 6.86 (d, 1H, $J$ = 8.0 Hz), 6.91 (1H, d, $J$ = 8.0 Hz), 7.07 (1H, s). $[\alpha]_D$ –16.2° ($c$ 0.10, MeOH, 16 °C).

*Synthesis of Aβ42*

The Aβ42 were synthesized in a stepwise fashion on 0.1 mmol of preloaded Fmoc-L-Ala-PEG-PS resin using a Pioneer™ Peptide Synthesizer as reported previously.[90] The Fmoc group was deblocked with 20% piperidine in DMF for 5 min (flow rate; 5.0 mL/min). The coupling reaction was carried out using Fmoc amino acid (0.4 mmol), HATU (0.4 mmo), and DIEPA (0.8 mmol) in DMF for 30 min (flow rate; 30 mL/min). After each coupling reaction, the N-terminal Fmoc group was removed with 20% piperidine in DMF. After the chain elongation was completed, the peptide-resin was treated with a cocktail containing trifluoroacetic acid, *m*-cresol, thioanisol, and 1,2-ethanedithiol for final deprotection and cleavage from the resin. The crude peptide was precipitated by diethylether and purified by HPLC on Develosil ODS UG-5 column (20 mm i.d. x 150 mm; Nomura Chemical Co., Seto, Aichi, Japan) using 80 min liner gradient of 10-50% $CH_3CN/H_2O$ containing 0.1% $NH_4OH$, described previously.[82] After lyophilization, the corresponding pure Aβ42 peptide was obtained, the purity of which was confirmed by HPLC (>98%). The molecular weight of Aβ42 was confirmed by MALDI-TOF-MS; Aβ42 ($m/z$, calcd: 4515.14, found: 4515.25 $[M+H]^+$)

*Thioflavin-T fluorescence assay*

The aggregative ability of Aβ42 was evaluated at 37 °C by the thioflavin-T (Th-T) method developed by Naiki *et al.*[91] The procedure was described elsewhere.[82] In brief, Aβ42 was dissolved in 0.1% $NH_4OH$ at 250 μM, and each flavonoid was dissolved in EtOH at 5.0 mM, followed by dilution with sodium phosphate-buffered saline (PBS: 50 mM sodium phosphate and 100 mM NaCl, pH 7.4) at the desired concentration (Aβ42, 25 μM; flavonoids, 50 μM). After incubation at 37 °C, 2.5 μL of each Aβ42 solution was added to 250 μL of 5.0 μM Th-T in 5.0 mM Gly-NaOH (pH 8.5). Fluorescence intensity was measured at 420 nm excitation and 485 nm emission using a micro-plate reader (MPR-A4ιII or Fluoroskan Ascent).

*Transmission electron microscopy (TEM)*

The aggregates of Aβ42 after a 48-h incubation were examined under a H-7650 electron microscope. The experimental procedure was described elsewhere.[82] In brief, each Aβ42 solution was prepared as described in Th-T assay and incubated at 37 °C for 48 h. After centrifugation at 4 °C for 10 min, the supernatant was removed from the pellets, and the aggregates were suspended in distilled water by gentle vortex mixing. The suspensions were applied to a 200-mesh Formvar-coated copper grid (Nissin EM, Tokyo, Japan) and dried in air before being

negatively stained for a few seconds with 2% uranyl acetate. The aggregates were examined with the H-7650 transmission electron microscope (Hitachi).

*Estimation of cell survival*

The reduction of 3-(4,5-dimethylthiazol-2-yl)-2,5-diphenyltetrazolium bromide (MTT) by mitochondrial reductase was carried out according to Shearman *et al*.[84] PC12 cells were cultured in Dulbecco's modified Eagle's medium (Sigma) containing 5% fetal calf serum, 10% horse serum, and 1% penicillin/streptomycin. Before using for the experiment, near-confluent culture of the cells were plated at approximately $10^4$ cells/100 μL/well in 96-well tissue culture plate coated with collagen, and incubated at 37 $^{o}$C under 5.0% $CO_2$ overnight. Aβ42 was dissolved in 0.1% $NH_4OH$ at 10 μM, and (+)-taxifolin was dissolved in DMSO at 1 mM, followed by dilution with flesh medium at the desired concentration (Aβ42, 1 μM; flavonoids, 10 μM). One hundred microlitters of the medium was exchanged with old one, and then the 96-well plate was incubated at 37 $^{o}$C under 5.0% $CO_2$. After 48-h incubation, 10 μL of 5 mg/mL MTT in PBS (pH 7.4) was added to the cell culture, which was incubated at 37 $^{o}$C under 5.0% $CO_2$ for 4 h. The culture medium was removed, and then 10% SDS/0.1 M $NH_4Cl$ (100 μL) was added to the cells. After further incubation overnight in the dark at room temperature, the absorbance at 595 nm was measured. The absorbance obtained by addition of vehicle was taken as 100%.

# Chapter 3

# Inhibitory mechanism for Aβ42 aggregation by catechol-type flavonoids*

## Introduction

Many researchers have reported protective effects of various polyphenols from green tea, turmeric, and red wine *etc*., against Aβ aggregation and neurotoxicity.[49-51] Several compounds [*e.g.* (–)-epigallocatechin-3-gallate (EGCG), curcumin, and resveratrol] are in clinical or preclinical trials for AD treatment.[47,66] However, the recent failures of some trials[33] motivated the author to clarify the mechanism by which polyphenols inhibit the aggregation of Aβ42 to develop promising leads for clinical use.

As mentioned in Chapter 2, the author isolated (+)-taxifolin,[80] a flavanonol which has a catechol moiety on the B-ring, as one of the active components in silymarin against Aβ42 aggregation (Fig. 8 in Chapter 2). Altough the catechol moiety on B-ring was suggested to be important for the anti-aggregative ability, the mechanism how the catechol moiety contributes to the activity is not fully understood. This Chapter describes a comprehensive study on the role of autoxidation of (+)-taxifolin in the prevention of aggregation and β-sheet transformation of Aβ42, and the effects of various flavanonols and flavonols on the aggregation of Aβ42 mutants substituted at Arg5, Lys16, and/or Lys28 with norleucine (Nle). The experiments using liquid chromatography-mass spectrometry (LC-MS) were also carried out to propose a site-specific inhibitory mechanism for Aβ42 aggregation by catechol-type flavonoids.

---

*The content described in this Chapter was originally published in *Journal of Biological Chemistry*. Mizuho Sato, Kazuma Murakami, Mayumi Uno, Yu Nakagawa, Sumie Katayama, Ken-ichi Akagi, Yuichi Masuda, Kiyonori Takegoshi and Kazuhiro Irie: Site-specific inhibitory mechanisms for amyloid-β42 aggregation by catechol-type flavonoids targeting the Lys residues. *J. Biol. Chem.* 2013; 288: 23212-23224. © The American Society for Biochemistry and Molecular Biology.

## Results

*Effects of autoxidation of (+)-taxifolin on its ability to prevent the aggregation of Aβ42*

A catechol moiety is easily oxidized to form an *o*-quinone.[92,93] To investigate the contribution of autoxidation to the inhibitory ability, the author examined the aggregative ability of Aβ42 in the presence of (+)-taxifolin treated with sodium periodate ($NaIO_4$), which is known as a mild oxidant of catechol but affecting little effect on peptide bond.[94] As shown in Fig. 11A, $NaIO_4$ extensively promoted the suppressive ability of (+)-taxifolin compared with (+)-taxifolin alone. These observations were also confirmed by the TEM experiment (Fig. 12A). $NaIO_4$ treatment in the presence of (+)-taxifolin formed only shorter and thinner fibrils compared with (+)-taxifolin alone. Aβ42 formed the typical fibrils even in the presence of $NaIO_4$ alone, and almost no differences (*e.g.* length, thickness) were observed between the morphology in the presence and absence of $NaIO_4$ (Fig. 12A).

$NaIO_4$ alone slightly affected the Th-T fluorescence of Aβ42 aggregates (Fig. 11A) possibly because $NaIO_4$ can oxidize Met35 in Aβ42 to its sulfoxide, the formation of which was confirmed by HPLC (Fig. 11E) and MALDI-TOF-MS (Aβ42-M35$^{ox}$; *m/z*: calcd: 4531.14, found: 4531.55 $[M+H]^+$). This is in good agreement with a report that oxidation using hydrogen peroxide, a strong oxidant, reduced Aβ42 aggregation.[95] However, in the presence of both (+)-taxifolin (50 μM) and $NaIO_4$ (100 μM), Met35 was not oxidized by $NaIO_4$; this was confirmed by HPLC (Fig. 11E) and MALDI-TOF-MS (Aβ42-M35$^{red}$; *m/z*: calcd: 4515.14, found: 4516.26 $[M+H]^+$). This indicates that $NaIO_4$ preferred to oxidize (+)-taxifolin more than the sulfur atom of the Met35 of Aβ42.

In addition, the author tested whether the treatment of $NaIO_4$ leads to the oxidation of Met35 in the preformed Aβ42 fibrils. The fibrils (*ca*. 28 μg) treated with $NaIO_4$ for 4 h were dissolved in formic acid (10 μL), and were sonicated for 1 h. After volatilization, the resultant pellets were resolved in 50% acetonitrile containing 0.1% trifluoroacetic acid, followed by subjection to MALDI-TOF-MS analysis. $NaIO_4$ did not oxidize Met35 in the preformed Aβ42 fibril (Aβ42-M35$^{red}$; *m/z*: calcd: 4515.14, found: 4515.12 $[M+H]^+$). Also in Th-T assay, Aβ42 fibril was not disassembled by $NaIO_4$

(data not shown). These mean that $NaIO_4$ could partially oxidize Met35 in the monomeric Aβ42, but not the fibrils.

Furthermore, in order to investigate the role of autoxidation, the effect by (+)-taxifolin on Aβ42 aggregation was tested *in vacuo*. Notably, (+)-taxifolin little suppressed the aggregation of Aβ42 under an anaerobic condition (Fig. 11B). In TEM images, typical fibril formation was observed even in the presence of (+)-taxifolin under the anaerobic condition (Fig. 12A). Aβ42 also aggregated in the presence of (+)-taxifolin and tris(2-carboxy-ethyl)phosphine (TCEP), a reductant (Fig. 11C). These results strongly suggest the autoxidation of (+)-taxifolin to be required for inhibitory activity against Aβ42 aggregation.

As mentioned in Chapter 1, the mechanism of Aβ42 fibril formation is well explained by a nucleation-dependent polymerization model mainly consisted of nucleation phase and extension phase.[11,12] To determine which stage (nucleation phase or extension phase) is affected by (+)-taxifolin, the author examined the effect of (+)-taxifolin on Aβ42 aggregation in the presence of the fibril seed as a template, according to the protocol developed by Naiki *et al.*[91] There was a nucleation phase (~1 h) when Aβ42 was incubated alone, whereas addition of the seeds skipped the nucleation phase, resulting in the rapid formation of Aβ42 fibrils (Fig. 11D). In the case of co-incubation of (+)-taxifolin with the seeds, the nucleation phase of Aβ42 did not drastically change, but the fluorescence gradually decreased after incubation for 4 h, suggesting that (+)-taxifolin could prevent the elongation phase (~2 or 4 h) in Aβ42 aggregation, rather than the nucleation phase (~1 h) (Fig. 11A, D). Although the slight difference of the length of elongation phase between Fig. 11A and 11D might be deduced from several factors, for example, outside temperature, batch (lot) of Aβ42, 2~4 h as an averaged time for elongation phase were observed in another independent experiments. Moreover, (+)-taxifolin destabilized the preformed Aβ42 fibril. The disappearance of nucleation phase in the presence of seed and $NaIO_4$ (Fig. 11D) implied the ability of oxidized taxifolin to disassemble even the seed. Indeed, the fluorescence of preformed Aβ42 fibrils immediately disappeared after addition of (+)-taxifolin treated with $NaIO_4$ (data not shown).

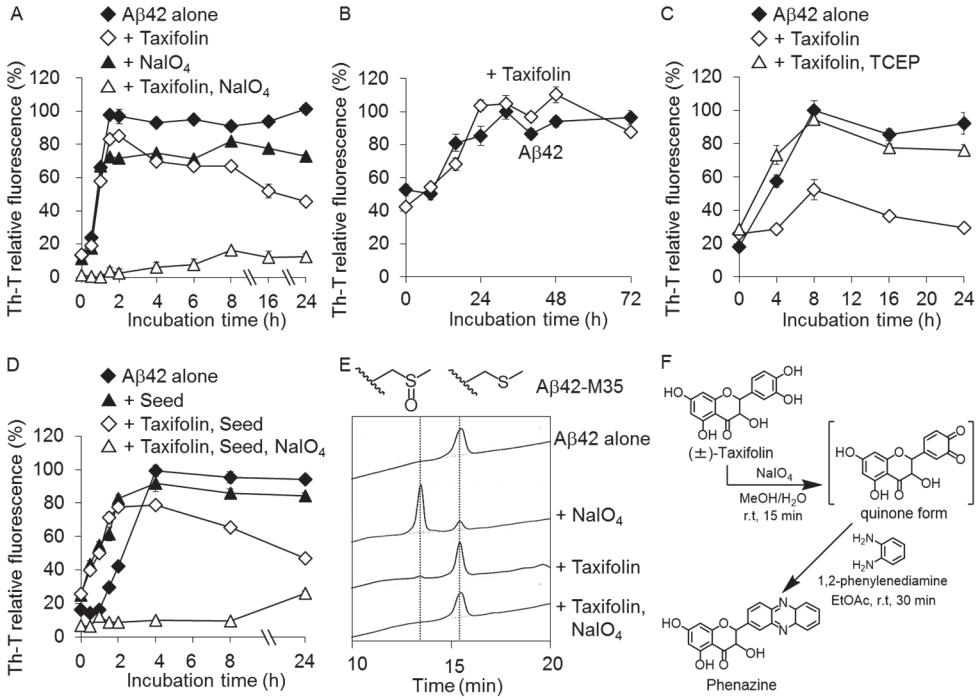


**Figure 11** (A) The effect of $NaIO_4$, an oxidant, on Aβ42 aggregation estimated by Th-T tests. Aβ42 (25 μM) was incubated with or without (+)-taxifolin (50 μM) and/or $NaIO_4$ (100 μM) in PBS (50 mM sodium phosphate, 100 mM NaCl, pH 7.4) at 37 °C. (B) The ability of (+)-taxifolin to suppress the aggregation of Aβ42 under an anaerobic condition. Aβ42 (25 μM) was incubated with or without (+)-taxifolin (50 μM) in PBS *in vacuo* at room temperature. (C) The effect of TCEP, a reductant, on Aβ42 aggregation. Aβ42 (25 μM) was incubated with or without (+)-taxioflin (50 μM) and/or TCEP (100 μM) in PBS at 37 °C. (D) The aggregative ability of Aβ42 in the presence of Aβ42 seed and/or (+)-taxifolin, $NaIO_4$. Aβ42 (25 μM) was incubated with or without the seed (10 μg/mL) and/or (+)-taxifolin (50 μM), $NaIO_4$ (100 μM) in PBS at 37 °C. The data are presented as the mean ± s.e.m. ($n$ = 8). Th-T relative fluorescence was expressed as a percentage of the fluorescence for wild-type Aβ42 alone, whose maximum value was taken as 100%. (E) HPLC analysis of Aβ42 solution with the indicated treatment. Aβ42 (25 μM) was incubated with or without (+)-taxifolin (50 μM) and/or $NaIO_4$ (100 μM) in PBS at 37 °C for 4 h. An aliquot was centrifuged by 20,130 *g* at 4 °C for 10 min, and the supernatant was subjected to HPLC on a Develosil ODS UG-5 column under a gradient of 10-50% $CH_3CN$ containing 0.1% $NH_4OH$ for 40 min. (F) Detection of *o*-quinone form of (+)-taxifolin using 1,2-phenylenediamine.

Next, the author measured UV spectra of (+)-taxifolin incubated with Aβ42 to evaluate the effects of $NaIO_4$ or the anaerobic condition on the autoxidation of (+)-taxifolin. When Aβ42 was incubated with (+)-taxifolin under air, the intensity of the peak at 260 nm and 400 nm gradually increased, and that of the peak at 320 nm decreased during 48 h of incubation (Fig. 12B). These spectral changes are characteristic of the oxidation of catechol-type flavonoids to form the *o*-quinone structure.[96] The addition of $NaIO_4$ accelerated these UV changes (Fig. 12B). In contrast, there was almost no changes in the UV spectra when (+)-taxifolin and Aβ42 were co-incubated *in vacuo* or with TCEP (Fig. 12B). These results indicate that the *o*-quinone formation in (+)-taxifolin through autoxidation plays a critical role in the inhibition of Aβ42 aggregation. The UV spectra of Aβ42 alone remained almost constant during the incubation (data not shown), meaning that the spectra of Aβ42 itself did not affect those of (+)-taxifolin.

Conversion to the *o*-quinone from (±)-taxifolin in the presence of $NaIO_4$ was also verified by reacting with *o*-phenylenediamine to yield phenazine (Fig. 11F), whose structure was confirmed by $^1$H NMR and HR-EI-MS. These data confirm the presence of *o*-quinone in (±)-taxifolin.

*Effects of autoxidation of (+)-taxifolin on its ability to inhibit transformation of a random structure into a β-sheet in Aβ42*

The effects of autoxidation of (+)-taxifolin on the secondary structure of Aβ42 was investigated by using CD spectroscopy. Shown in Fig. 13 is the data for Aβ42; the positive peak at 195 nm and negative peak at 215 nm drastically increased even after 4 h of incubation, and remained until 48 h of incubation, suggesting that a random structure transformed into a β-sheet in Aβ42 (Fig. 13A). On the other hand, (+)-taxifolin strongly delayed the transformation of Aβ42 (Fig. 13B). Furthermore, addition of $NaIO_4$ decelerated the transformation process during 0~8 h (Fig. 13C).

The author also measured the CD spectra under an anaerobic condition (Fig. 13D, E). A spectrum related to the β-sheet formation was found only after 24 h of incubation, but its peak intensity was weaker than that of Aβ42 under air in Fig. 13A. Since radicalization of Aβ42 induced by reactive oxygen species is indispensable to its aggregation,[22] these results seem to be reasonable. The transformation into a β-sheet was not suppressed either by (+)-taxifolin *in vacuo*. The findings suggest that the effects of autoxidation

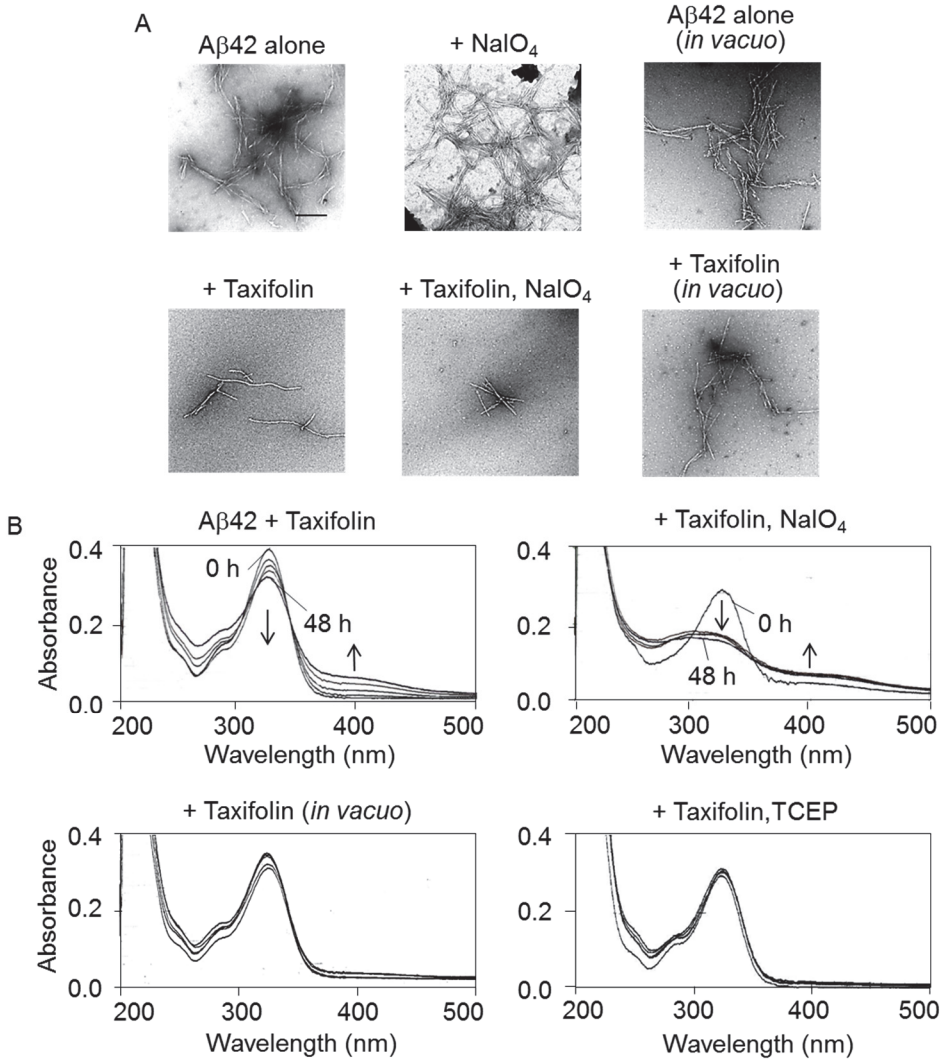


**Figure 12** (A) TEM images of Aβ42 aggregates after 48 h of incubation. Aβ42 (25 μM) was treated with or without (+)-taxifolin (50 μM) and/or $NaIO_4$ (100 μM) in PBS under an aerobic or anaerobic condition. Scale bar, 200 nm. (B) UV-visible spectra of (+)-taxifolin (50 μM) treated with Aβ42 (25 μM) in the presence of $NaIO_4$ or TCEP (100 μM) in PBS after incubation for 0, 4, 8, 24, and 48 h, respectively.

of (+)-taxifolin on its ability to inhibit Aβ42 aggregation are closely associated with prevention of the transformation into a β-sheet.

*LC-MS analysis of Aβ42 treated with oxidized taxifolin*

The *o*-quinone of flavonoids can form covalent bonds with nucleophilic residues in proteins (*e.g.* Cys, Arg, Lys) to modulate their activity.[97] Because Aβ42 has three basic amino acid residues (Arg5, Lys16, and Lys28), the author asked if these residues bound to oxidized taxifolin covalently. The *o*-quinone derived from (+)-taxifolin can react with Lys or Arg residues in Aβ42 through a Michael addition or Schiff base formation (Fig. 14A).

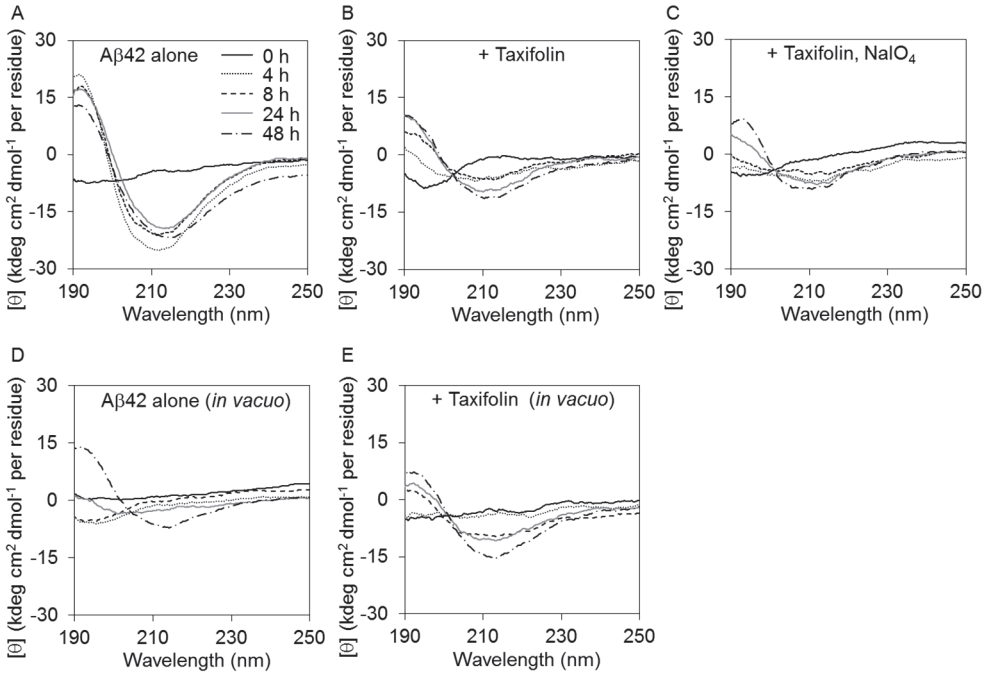


**Figure 13** Effects of autoxidation of (+)-taxifolin on its ability to prevent the transformation into the β-sheet structure of Aβ42 using CD spectrometry. (A-C) Aβ42 (25 μM) was incubated (A) without, with (+)-taxifolin (50 μM) in the (B) absence or (C) presence of $NaIO_4$ (100 μM) at 37 °C for the period indicated. (D and E) Aβ42 (25 μM) was incubated (D) without or (E) with (+)-taxifolin (50 μM) *in vacuo* at room temperature for the period indicated.

An Aβ42 solution incubated with (+)-taxifolin and $NaIO_4$ for 4 h was analyzed using a highly sensitive ion trap type LC-MS equipped with a TOF mass analyzer (LCMS-IT-TOF). As shown in Fig. 14B, LC-MS measurements gave the mass envelop at +7, +6, and +5 charge distribution (deconvoluted mass: 4817.12, calcd: 4816.38), corresponding to the Aβ42–oxidized taxifolin adduct resulted from Michael addition. These results imply that the basic amino acid residues of Aβ42 might be involved in the covalent bonding with the oxidized taxifolin.

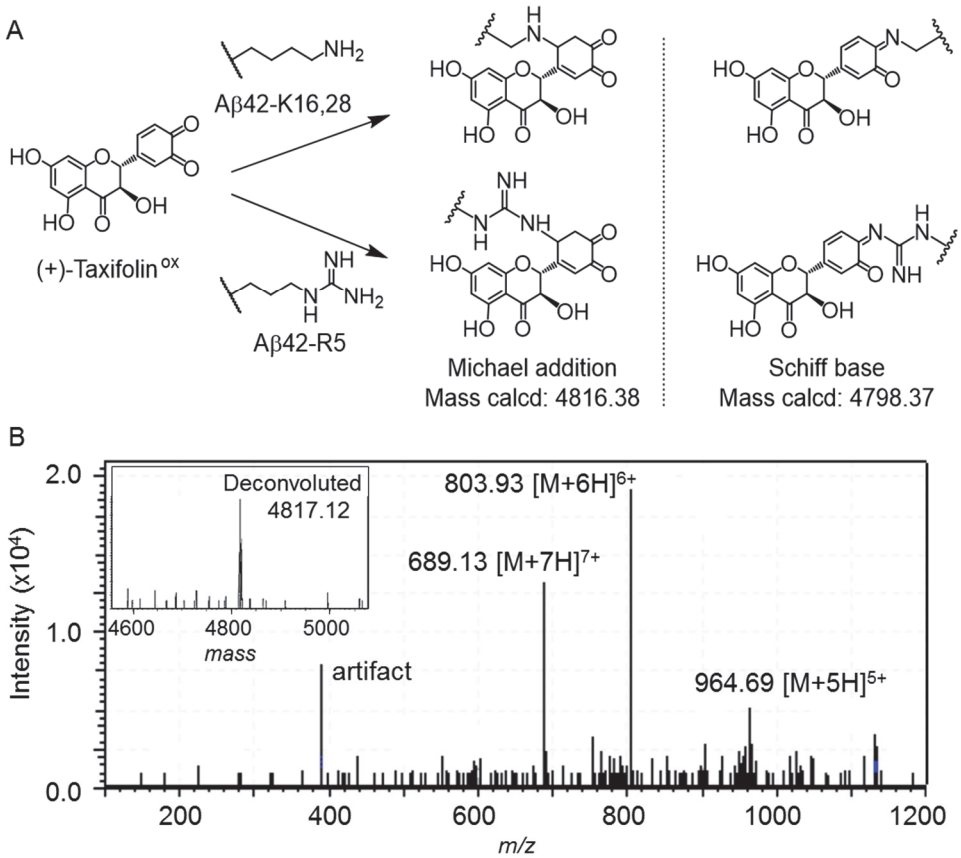


**Figure 14** (A) The proposed structures of adducts of Aβ42 with oxidized taxifolin. (upper) Lys16, Lys28, and (lower) Arg5 in Aβ42 could attack the *o*-quinone of (+)-taxifolin, resulting in (left) Michael addition or (right) Schiff base formation with the indicated calculated mass. (B) LCMS-IT-TOF analysis of the Aβ42 solution treated with oxidized taxifolin. After Aβ42 (25 μM) was incubated with (+)-taxifolin (50 μM) in the presence of $NaIO_4$ (100 μM) in PBS at 37 °C for 4 h, an aliquot was subjected to the analysis

*Inhibitory effect of (+)-taxifolin on aggregation of Aβ42 mutants substituted at Arg5, Lys16, and/or Lys28*

Although formation of Michael adducts between the *o*-quinone of (+)-taxifolin and the Lys residues of Aβ42 was suggested in LC-MS (Fig. 14B) together with the verification of the *o*-quinone formation (Fig. 11F), an attempt to determine the Lys residues involved in the adduct formation by LC-MS/MS analysis was disappointing, possibly because of the extremely low amount and/or instability of the adduct. To obtain further insight into the mechanism by which (+)-taxifolin inhibits the aggregation of Aβ42, we prepared five Aβ42 mutants [R5Nle-, K16Nle-, K28Nle-, K16,K28$(Nle)_2$-, and R5,K16,K28$(Nle)_3$-Aβ42], where the basic amino acid residues of Aβ42 were substituted with norleucine (Nle). The aggregative ability in the presence or absence of (+)-taxifolin was also estimated (Fig. 15A-E). These mutants retained substantial aggregative abilities to form fibrils (70~80%) compared with wild-type Aβ42 in Th-T test (Fig. 15F). (+)-Taxifolin did not suppress the aggregative ability of K16Nle-Aβ42 (Fig. 15B). K28Nle-Aβ42 also aggregated in the presence of (+)-taxifolin, though intensity of the Th-T fluorescence slightly decreased than that for K28Nle-Aβ42 alone (Fig. 15C). Moreover, (+)-taxifolin did not prevent the aggregation of K16,K28$(Nle)_2$-Aβ42 and R5,K16,K28$(Nle)_3$-Aβ42 (Fig. 15D, E). On the other hand, (+)-taxifolin largely suppressed the aggregation of R5Nle-Aβ42 (Fig. 15A). These results indicate that adduct formation with lysine residues at positions 16 and 28 have an important role in prevention of the Aβ42 aggregation. More correctly, since the aggregative ability of K28Nle-Aβ42 was slightly suppressed by (+)-taxifolin compared with that of K16Nle-Aβ42 (Fig. 15B, C), Lys16 would be more effective target than Lys28 in inhibition of Aβ42 aggregation.

*Inhibition of Aβ42 aggregation by non-catechol-type flavonoids*

Almost the flavonoids (myricetin, quercetin, morin, and kaempferol), which were previously reported to inhibit Aβ42 aggregation,[12)] belong to the flavonols. Flavonols contain a double bond between C2 and C3 on the C-ring, whereas flavanonols like (+)-taxifolin do not (Fig. 16). To obtain the insight into the inhibitory mechanism for Aβ42 aggregation by flavonols as well as flavanonols, the author evaluated the effects of these compounds on Aβ42 aggregation. The $IC_{50}$ was calculated for Aβ42 aggregation from

the inhibitory rate (%) of each flavonoid [10, 25, 50, 100 μM for a strong-class inhibitor (dihydromyricetin, (+)-taxifolin, myricetin, quercetin); 25, 50, 100, 250 μM for a middle-class inhibitor (morin, kaempferol, datiscetin); 50, 100, 250, 500 μM for a weak-class inhibitor (dihydrokaempferol, pinobanksin, galangin)] on the aggregation of Aβ42 (25 μM) after a 24-h incubation (Fig. 16).

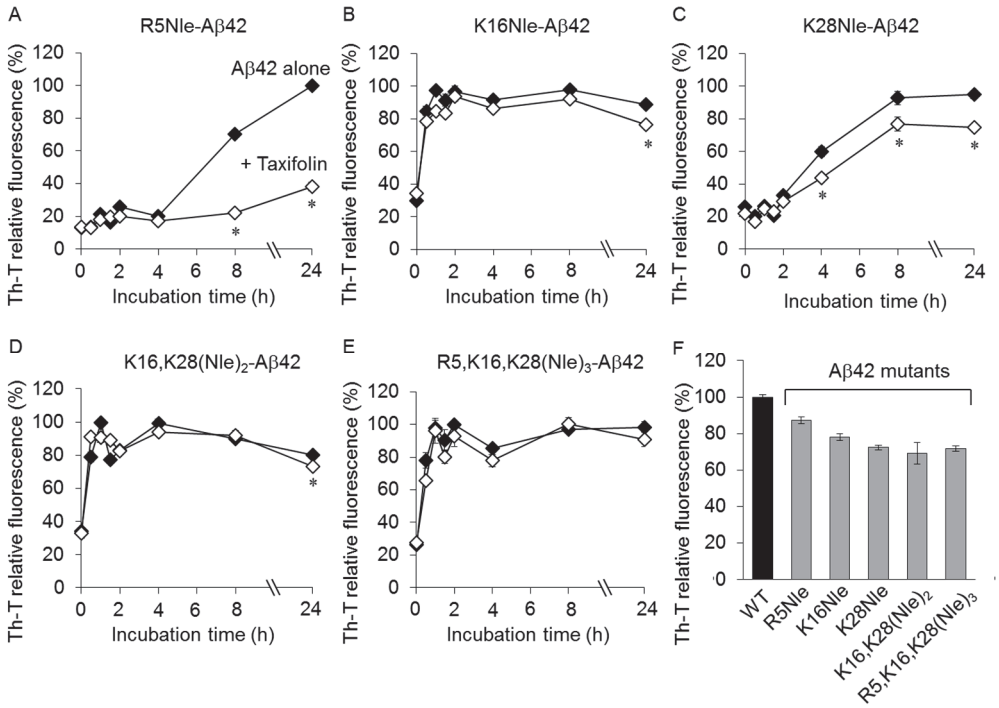


**Figure 15** The aggregative ability of (A) R5Nle-Aβ42, (B) K16Nle-Aβ42, (C) K28Nle-Aβ42, (D) K16,K28(Nle)$_2$-Aβ42, and (E) R5,K16,K28(Nle)$_3$-Aβ42 in the presence of (+)-taxifolin was examined by Th-T assay. Each Aβ42 mutant (25 μM) was incubated with or without (+)-taxifolin (50 μM) in PBS at 37 °C. ◆, Aβ42mutant without flavonoid; ◇, Aβ42 mutant with (+)-taxifolin. The data are presented as the mean ± s.e.m. ($n$ = 8). Th-T relative fluorescence was expressed as a percentage of the fluorescence for Aβ42 mutant alone, whose maximum value was taken as 100%. *$p$ < 0.05 compared with Aβ42 mutant alone. The time point without asterisk means no significant difference between Aβ42 mutant treated and untreated with (+)-taxifolin. (F) The comparison of aggregative ability of Aβ42 mutants. Th-T relative fluorescence of each mutant after incubation for 24 h was expressed as a percentage of the fluorescence for wild-type Aβ42 alone, whose maximum value was taken as 100%. The data are presented as the mean ± s.e.m. ($n$ = 8).

Among flavanonols, dihydromyricetin ($IC_{50}$ = 25.3 μM) as well as (+)-taxifolin ($IC_{50}$ = 33.0 μM) with contiguous hydroxyl groups on the B-ring suppressed the aggregation of Aβ42, whereas dihydrokaempferol and pinobanksin ($IC_{50}$ >500 μM) with one or no hydroxyl group did not (Fig. 16), suggesting vicinal hydroxyl groups on the B-ring to be essential for the inhibitory activity of flavanonols. Similarly, among flavonols, the author compared the ability to inhibit Aβ42 aggregation of myricetin, quercetin, morin, kaempferol, datiscetin, and galangin. The aggregation of Aβ42 was strongly suppressed by myricetin ($IC_{50}$ = 15.1 μM) and quercetin ($IC_{50}$ = 15.3 μM) with vicinal hydroxyl groups on the B-ring, while galangin ($IC_{50}$ >500 μM) without a hydroxyl group on the B-ring did not show any inhibitory activity (Fig. 16). Interestingly, morin ($IC_{50}$ = 30.3 μM), kaempferol ($IC_{50}$ = 75.1 μM), and datiscetin ($IC_{50}$ = 55.4 μM) without a catechol moiety moderately suppressed the aggregation of Aβ42.

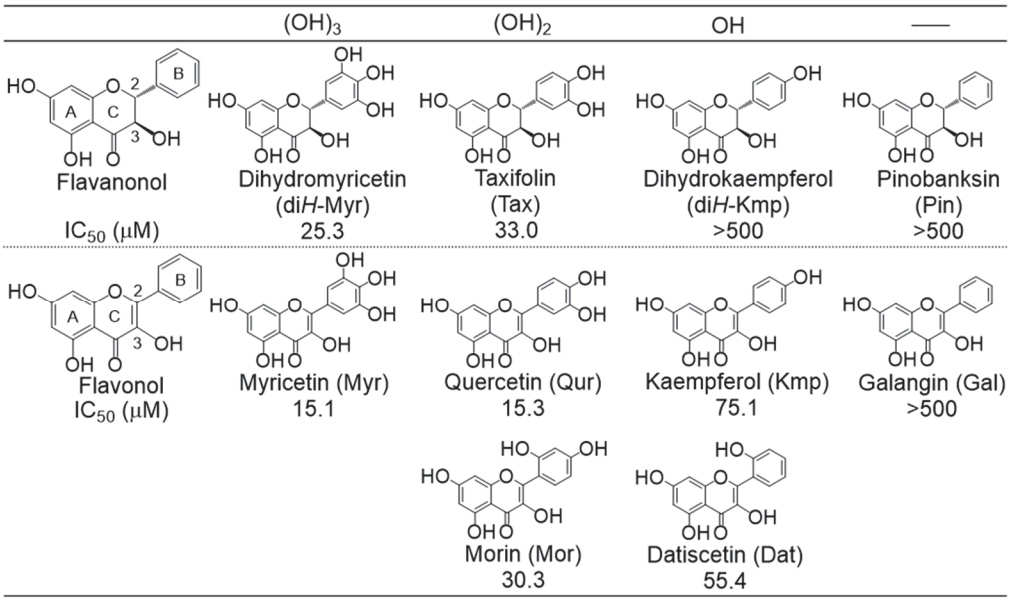


**Figure 16** The structures and $IC_{50}$ values of (upper) flavanonols and (lower) flavonols examined in this study. The $IC_{50}$ value was calculated from the inhibitory rate (%) of each flavonoid on Aβ42 (25 μM) aggregation after 24 h incubation using Th-T assay.

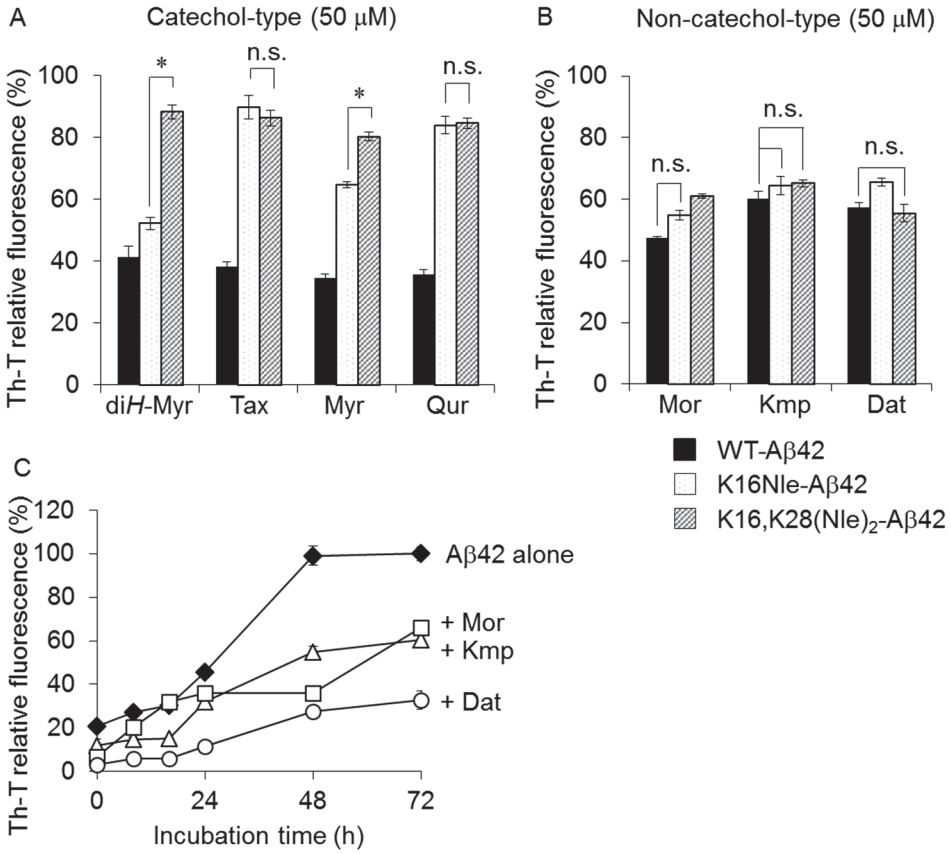


**Figure 17** (A) The aggregative ability of Aβ42 mutants incubated with a catechol-type flavanonol or flavonol for 24 h estimated by Th-T tests. Each Aβ42 mutant (25 μM) was incubated with or without (+)-taxifolin (50 μM) in PBS at 37 °C. The data are presented as the mean ± s.e.m. ($n$ = 8). Th-T relative fluorescence was expressed as a percentage of the fluorescence for each Aβ42 alone, whose value at 24 h was taken as 100%. (B) The aggregative ability of Aβ42 mutants (25 μM) treated with a non-catechol-type flavonol (50 μM) for 24 h, estimated by Th-T tests. *$p < 0.05$. n.s. = not significant. (C) The effect of non-catechol-type flavonoids (50 μM) on Aβ42 (25 μM) aggregation *in vacuo*. Th-T relative fluorescence was expressed as a percentage of the fluorescence for Aβ42 alone, whose maximum value was taken as 100%.

To gain further insight into the mechanism by which flavonoids inhibit Aβ42 aggregation by targeting the Lys residues, aggregation tests were carried out in the presence of catechol-type flavonoids (dihydromyricetin, (+)-taxifolin, myricetin or quercetin), or non-catechol-type flavonols (morin, kaempferol, or datiscetin) using K16Nle- and K16,K28$(Nle)_2$-Aβ42. The author compared the aggregative ability of Aβ42 mutant incubated with each flavonoid, the concentration of which was the maximal value to suppress the fluorescence of Aβ42 under 50% by (+)-taxifolin (data not shown). The catechol-type (+)-taxifolin and quercetin did not suppress the aggregation of these Aβ42 mutants. Although dihydromyricetin and myricetin with contiguous trihydroxyl groups significantly prevented the aggregation of K16Nle-Aβ42, these flavonoids did not change the aggregative potency of K16,K28$(Nle)_2$-Aβ42 (Fig. 17A), implying that they could react with Lys28 as well as Lys16 because contiguous trihydroxyl groups might facilitate the autoxidation of the B-ring compared with (+)-taxifolin and quercetin containing vicinal hydroxyl groups.

Notably, in the case of non-catechol-type flavonols (morin, kaempferol, and datiscetin), there was little difference in the inhibitory activity among the wild-type, K16Nle-Aβ42, and K16,K28$(Nle)_2$-Aβ42 (Fig. 17B). Regarding the relevance of autoxidation to the inhibition of Aβ42 aggregation, the Th-T fluorescence of Aβ42 treated with these three non-catechol-type flavonols under an anaerobic condition was measured. All these flavonols suppressed the aggregation of Aβ42 even *in vacuo* (Fig. 17C), indicating that the inhibition of non-catechol-type flavonols could not be ascribed to their autoxidation. These results suggest the existence of another inhibitory mechanism for Aβ42 aggregation by non-catechol-type flavonols, which will be discussed in Chapter 4.

## Discussion

Thus far, the anti-AD activity of flavonoids has been believed to originate from their anti-oxidative activity and/or β-sheet recognition due to their hydrophobicity and planarity. However, these parameters are not necessarily accompanied by the ability to inhibit the aggregation of Aβ42 and other amyloidogenic proteins.[49] This background led us to reconsider whether the inhibitory activity can be simply explained by these "less-specific" properties (anti-oxidation, hydrophobicity, and planarity) or not.

On the basis of the present results, the author propose a site-specific mechanism whereby catechol-type flavonoids inhibit the aggregation of Aβ42, in which a catechol structure could be autoxidized to form the *o*-quinone on the B-ring, followed by the formation of the *o*-quinone-Aβ42 adduct targeting Lys residues at positions 16 and 28 of Aβ42, but not be originated from the anti-oxidative activity (Fig. 18). This could provide unique opportunities to design potent inhibitors of Aβ42 aggregation. On the other hand, the inhibitory ability of non-catechol-type flavonols

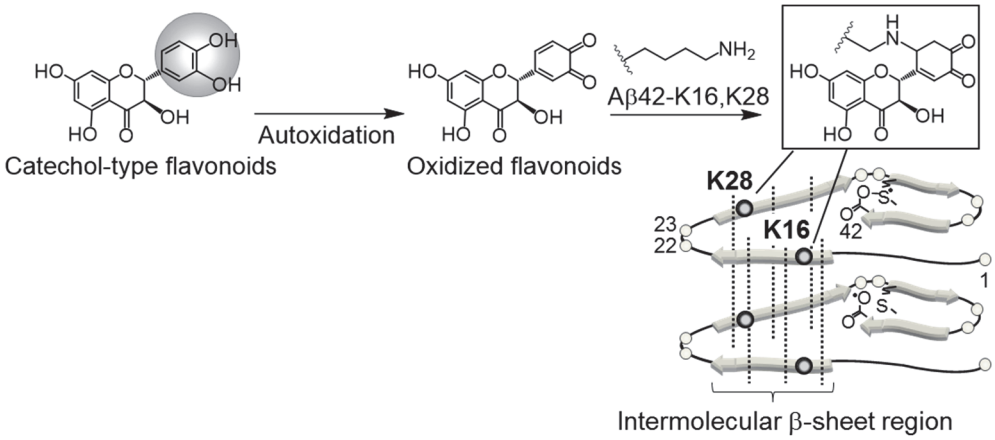


**Figure 18** Site-specific inhibitory mechanisms of Aβ42 aggregation by catechol-type flavonoids. Catechol-type flavanonols (*e.g.* (+)-taxifolin) or flavonols were oxidized to form corresponding *o*-quinones on B-ring, followed by the formation of adducts by Lys16 and Lys28 of Aβ42. Because Lys16 and Lys28 are incorporated in the intermolecular β-sheet region, Aβ42 aggregates would be destabilized by the adduct formation.

containing a double bond between C2 and C3 on the C-ring (Fig. 16) does not require the autoxidation. The data in Figs. 16 and 17 indicate that the interaction of non-catechol-type flavonols with Aβ42 might be less effective than the conjugate addition of the Lys residues to the *o*-quinone moiety derived from autoxidation. These findings might explain in part the difference in the inhibitory ability between flavanonols and flavonols.

Previous investigation using solid-state NMR by Masuda *et al.*[98] together with systematic proline replacement identified a toxic conformer with a turn at positions 22 and 23 in Aβ42, and proposed that the residues at positions 15-21 and 24-32 containing Lys 16 and Lys 28 are involved in the intermolecular β-sheet region, whereas the N-terminal 13 residues are not.[99] A monoclonal antibody against the toxic turn at positions 22 and 23 detected Aβ oligomers in human AD brain[100] and induced pluripotent stem cells[101] as well as in AD mice.[102,103] As mentioned above, an attempt to determine the

Recently, Bitan's group reported that the Lys-specific synthetic compound (molecular tweezer, CLR01) prevented the cytotoxicity and oligomerization of Aβ42 through non-covalent interaction *in vitro*[43] and *in vivo*.[44] Their subsequent study using Aβ42 mutants substituted at Lys16 or Lys28 with Ala revealed a key role for Lys residues in Aβ42-induced neurotoxicity rather than aggregation.[104] These reports did not contradict the results that the aggregates of double and triple mutants [K16,K28(Nle)$_2$-Aβ42 and R5,K16,K28(Nle)$_3$-Aβ42] after 24-h of incubation were slightly less than that of wild-type Aβ42 in this study (Fig. 15F).

R5Nle-Aβ42 (~4 h) and K28Nle-Aβ42 (~2 h) had the nucleation phase (Fig. 15A, C), while three Aβ42 mutants [K16Nle-Aβ42, K16,K28(Nle)$_2$-Aβ42, and R5,K16,K28(Nle)$_3$-Aβ42] including the substitution of K16 with Nle did not (Fig. 15B, D, E). These mean that the aggregative ability of K16Nle-Aβ42 seems to be more potent than that of K28Nle-Aβ42. Because Lys16 residue is located at a hydrophobic cavity in the β-sheet region,[105] the substitution with norleucine without an amino group could enhance the hydrophobic interaction in Aβ42 aggregates, leading to passing the nucleation phase. In contrast, Lys28 was involved in the formation of salt bridge between Asp23 and Lys28 for Aβ42 aggregation.[105] These findings imply the different role of lysine resides at positions 16 and 28 in Aβ42 aggregation, which might explain the difference of aggregative ability between K16Nle- and K28Nle-Aβ42.

Notably, the nucleation phase of R5Nle-Aβ42 (~4 h) was partially longer than that of wild-type Aβ42 (~1 h) (Figs. 11A, D, and 15A). Since the flexibility of N-terminal region has been thought to be essential for aggregation of Aβ42,[105] the replacement of Arg5 with norleucine might retard the nucleation phase in wild-type Aβ42 aggregation by increasing hydrophobic interaction. Moreover, given no nucleation phase of three Aβ42 mutants of Lys16, it is not surprising that (+)-taxifolin did not largely alter the aggregation properties of these mutants, because (+)-taxifolin could specifically target the elongation phase in wild-type Aβ42 aggregation targeting Lys16, rather than the nucleation phase.

LeVine *et al.*[106] suggested preventive effects on Aβ42 aggregation by several dihydroxybenzoic acid isomers, in which 2,3- and 3,4-dihydroxy benzoic acids delayed the velocity of oligomer formation. Fisetin, a quercetin analogue without the 5-OH group on the A-ring, also inhibited the aggregation of Aβ42.[86] Ushikubo *et al.*[65] reported that 7-OH group on the A-ring is not involved in the anti-aggregative ability of flavonols. These are consistent with the structure-activity relationship of (+)-taxifolin described in Chapter 2. On the other hand, lacmoid without a catechol moiety bound less-specifically to Aβ42.[107] These findings together with the present results strongly support that flavonoids with vicinal hydroxyl groups on the B-ring could be indispensable to bind covalently with Aβ42 to suppress its aggregation. It is also reasonable that 3,4,5-trihydroxybenzoic acid, gallic acid[106] and 3',4',5'-trihydroxyflavone[65] as well as dihydromyricetin (Fig. 16) suppressed the aggregation of Aβ42. In particular, the inhibitory activities of dihydromyricetin, (+)-taxifolin, myricetin, and quercetin were higher than those of morin, kampferol, and datiscetin (Fig. 16), suggesting that the nucleophilic addition to the *o*-quinone moiety by the Lys residues of Aβ42 could contribute more significantly to the inhibition of Aβ42 aggregation than the hydrophobic interaction. However, additional role of the A- and C-rings of catechol-type flavonoids in the suppression of Aβ42 aggregation is not negligible, since the inhibitory activity of catechol itself was low.[108]

Fink and colleagues previously proposed the contribution of interaction of Lys residues with the baicalein *o*-quinone to the inhibition of α-synuclein responsible for Parkinson's disease.[97] However, the underlying molecular mechanism cannot be fully explained by the oxidized baicalein because the aggregation of α-synuclein was inhibited by baicalein even under an

anaerobic condition.[97] Quite recently, the oxidation product of EGCG was in part involved in remodeling the preformed fibrils of Aβ40 by EGCG.[109]

Booth *et al*.[110] showed that (+)-taxifolin was not toxic when given long term to albino rats. Furthermore, it was reported that bioavailability of (+)-taxifolin after oral administration of lipid solution was 36% in rat plasma.[111] Although some polyphenols [quercetin,[112] naringenin[113] and curcumin[114]] were reported to pass through the blood-brain barrier after oral administration, caution should be used because of the difference between animal and clinical condition.

## Experimental procedures

*Synthesis of (+)-taxifolin, dihydrokaempferol and pinobanksin*

Synthesis of (+)-taxifolin was described in Chapter 2. (±)-Dihydrokaempferol[115)] and (±)-pinobanksin[116)] were synthesized in a manner similar to (±)-taxifolin using 4-hydroxybenzaldehyde or benzaldehyde in place of vanillin as a starting material, respectively (Scheme 1B in Chapter 2). Enantiomers were not separated because the inhibitory effect on Aβ42 aggregation by (–)-taxifolin was almost the same as that by (+)-taxifolin. The structure of each of these compounds was confirmed by $^1$H NMR and EI-MS. Other flavonoids; myricetin (Wako, Osaka, Japan), kaempferol, (±)-dihydromyricetin (ChromaDex, Irvine, CA), morin, galangin, quercetin (Sigma, St. Louis, MO), and datiscetin (Extrasynthese, Genay, France) were purchased commercially.

(±)-Dihydrokaempferol: $^1$H NMR (400 MHz, 297.9 K, acetone-$d_6$, 56.9 mM) δ 4.65 (1H, d, $J$ = 11.6 Hz), 5.08 (1H, d, $J$ = 11.6 Hz), 5.94 (1H, d, $J$ = 2.1 Hz), 5.99 (1H, d, $J$ = 2.0 Hz), 6.89 (2H, brd, $J$ = 8.6 Hz), 7.42 (2H, brd, $J$ = 8.5 Hz), 11.7 (1H, brs). EI-MS: *m/z*, calcd: 288, found: 288 $[M]^+$.

(±)-Pinobanksin: $^1$H NMR (400 MHz, 297.6 K, acetone-$d_6$, 16.9 mM) δ 4.68 (1H, d, $J$ = 11.6 Hz), 5.19 (1H, d, $J$ = 11.6 Hz), 5.98 (1H, d, $J$ = 2.1 Hz), 6.01 (1H, d, $J$ = 2.1 Hz), 7.39-7.47 (3H, m), 7.59-7.61 (2H, m), 11.7 (1H, brs). EI-MS: *m/z*, calcd: 272, found: 272 $[M]^+$.

*Trapping of the* o-*uiqnone form of (+)-taxifolin by phenylenediamine*

Sodium periodate ($NaIO_4$, 19 mg, 89 μmol) in $H_2O$ (0.20 mL) was added to (±)-taxifolin (28 mg, 91 μmol; Toronto Research Chemicals Inc. North York, ON, Canada) in methanol (3.5 mL). After stirring for 15 min at room temperature, the reaction mixture was extracted with ethyl acetate (5.0 mL), to which 1,2-phenylenediamine (9.8 mg, 91 μmol; Wako) was added before stirring for 30 min at room temperature. The mixture was concentrated and separated by HPLC on a YMC SH-342-5AL column (20 mm i.d. x 150 mm; YMC, Kyoto, Japan) with 60% MeOH/$H_2O$ to give the corresponding phenazine (3.8%) (Fig. 11F). The structure was confirmed by $^1$H NMR and high resolution (HR)-EI-MS. $^1$H NMR (500 MHz, 295.3 K, acetone-$d_6$, 6.98 mM) δ 4.87 (1H, d, $J$ = 11.5 Hz), 5.59 (1H, d, $J$ = 11.5 Hz), 6.07 (1H, s), 6.09 (1H, s), 7.96-8.00 (2H, m), 8.22 (1H, dd, $J$ = 9.0, 1.7 Hz), 8.26-8.30 (2H, m), 8.33 (1H, d, $J$ = 9.0 Hz), 8.46 (1H, d, $J$ = 1.7 Hz), 11.7 (1H, brs); HR-EI-MS *m/z* 374.0902 $[M]^+$, calcd for $C_{21}H_{14}N_2O_5$ 374.0903.

*Thioflavin-T fluorescence assay*

The aggregative ability of Aβ42 was evaluated at 37 °C by the thioflavin-T (Th-T) method developed by Naiki *et al.*[91)] See Chapter 2 for details. In brief, Aβ42 was dissolved in 0.1% $NH_4OH$ at 250 μM, and each flavonoid was dissolved in EtOH at 5 mM, followed by dilution with PBS (50 mM sodium phosphate and 100 mM NaCl, pH 7.4) at the desired concentration (Aβ42, 25 μM; flavonoids, 50 μM). $NaIO_4$ or Tris(2-carboxyethyl)phosphine hydrochloride (TCEP-HCl) was

initially dissolved in PBS at 100 mM, then diluted with PBS at 100 μM before use. Experiments under an anaerobic condition were performed in a desiccator evacuated by a diaphragm pump (*ca*. 8 mmHg; KNF Lab LABOPORT vacuum pump, KNF Neuberger, NJ) at room temperature. Unless otherwise noted, the concentrations of Aβ42, flavonoids, and oxidant/reductant used in this study were 25, 50, and 100 μM, respectively.

The effect of the addition of $NaIO_4$ on Met35 oxidation was estimated by HPLC on a Develosil ODS UG-5 column (6.0 mm i.d. x 100 mm; Nomura chemical, Seto, Japan) under a gradient of 10-50% $CH_3CN$ containing 0.1% $NH_4OH$ for 40 min after the centrifugation of the Aβ42 solution at 20,130 *g* at 4 °C (MX-300; TOMY, Tokyo, Japan) for 10 min.

The seeds of Aβ42 were also prepared basically according to the protocol developed by Naiki *et al.*[91] Briefly, after incubation of Aβ42 (25 μM) in PBS (pH 7.4) for 24 h at 37 °C, the pellet obtained by centrifugation at 20,130 *g* at 4 °C for 1 h was suspended by pipetting in PBS (pH 7.4) at concentration of 1 mg/mL. The resultant solution was sonicated for 1 h in an ultrasonic device (MUS-20; EYELA, Tokyo, Japan), followed by dilution with PBS at 10 μg/mL before use. Th-T relative fluorescence was expressed as a percentage of wild-type Aβ42 alone, whose maximum value was taken as 100%.

*Transmission electron microscopy (TEM)*

See Chapter 2

*UV-visible spectrometry*

Oxidation of (+)-taxifolin was monitored by UV spectroscopy (UV-2200A; Shimadzu). (+)-Taxifolin (50 μM) was incubated with Aβ42 (25 μM) in PBS (50 mM sodium phosphate and 100 mM NaCl, pH 7.4) at 37 °C. The solution was then loaded into a 1-cm path length quartz cell, and UV spectra were recorded at 200-500 nm. The sample was diluted three times with PBS because of its strong absorbance.

*Circular dichroism (CD) spectrometry*

The secondary structure of Aβ42 was estimated by CD spectrometry (J-805; JASCO, Tokyo, Japan) using a 0.1-mm quartz cell (121.027-QS, $\phi$ 10 mm; JASCO), as described elsewhere.[83] Aβ42 (25 μM) was incubated with or without (+)-taxifolin (50 μM) in PBS (50 mM sodium phosphate and 100 mM NaCl, pH 7.4) at 37 °C. An aliquot was loaded into the quartz cell, and CD spectra were recorded at 190-250 nm. Experiments under an anaerobic condition were performed as described before. The spectra of Aβ42 are shown after subtraction of the spectrum for vehicle alone, and those in the presence of (+)-taxifolin are shown after subtraction of the spectrum for (+)-taxifolin alone.

*LC-MS analysis*

Aβ42 solution (25 μM) was incubated with 50 μM (+)-taxifolin in PBS (50 mM sodium phosphate and 100 mM NaCl, pH 7.4) in the presence of 100 μM $NaIO_4$ at

37 $^{o}$C. After a 4-h incubation, the mixture was desalted and condensed twice by ZipTip C18 (Millipore, Bedford, MA). Five microliters of the solution was subjected to a liquid chromatography mass spectrometry ion trap time-of-flight (LCMS-IT-TOF; Shimadzu) through a YMC-Pack ODS-AQ column (6.0 mm i.d. x 100 mm; YMC) at 25 $^{o}$C under a gradient of 20-60% $CH_3CN$ containing 0.1% formic acid for 30 min.

*Synthesis of Aβ42 mutants*

Aβ42 mutants were synthesized in the same manner as described in Chapter 2 using Fmoc-norleucine (Nle)-OH in place of arginine or lysine, respectively. Fmoc-Nle-OH was purchased from Watanabe Chemical Industries (Hiroshima, Japan).

The molecular weight of each Aβ42 mutant was confirmed by MALDI-TOF-MS (AXIMA-CFR); R5Nle-Aβ42 (*m/z*, calcd: 4472.11, found: 4472.38 $[M+H]^+$), K16Nle-Aβ42 (*m/z*, calcd: 4500.12, found: 4500.25 $[M+H]^+$), K28Nle-Aβ42 (*m/z*, calcd: 4500.12, found: 4500.32 $[M+H]^+$), K16,K28$(Nle)_2$-Aβ42 (*m/z*, calcd: 4485.11, found: 4485.13 $[M+H]^+$), R5,K16,K28$(Nle)_3$-Aβ42 (*m/z*, calcd: 4442.08, found: 4442.58 $[M+H]^+$).

*Statistical analyses*

All data are presented as the means ± s.e.m. and the differences were analyzed with an one-way analysis of variance (ANOVA) followed by Bonferroni's test or unpaired Student's *t*-test. These tests were implemented within GraphPad Prism software (version 5.0d). $P$ values < 0.05 were considered significant.

# Chapter 4

# Solid-state NMR analysis of interaction sites between (+)-taxifolin and Aβ42

## Introduction

Curcumin, as well as (+)-taxifolin, has anti-amyloidogenic effect for Aβ, including fibril formation, extension, destabilization of preformed fibril, and oligomer formation.[54] It was mentioned that the binding of curcumin to Aβ is due to hydrophobicity and both the terminal phenyl groups from structure-activity relationship study.[57] Recent studies by Masuda *et al.*[69] using a solid-state NMR proposed that curcumin with an α,β-unsaturated ketone interacted with the aromatic hydrophobic core (Aβ17-21) due to its inherent hydrophobicity and planarity, resulting in the inhibition of Aβ42 aggregation *via* the intercalation (Fig. 20A).

On the other hand, as mentioned in Chapter 3, (+)-taxifolin, which is less planar but has catechol-moiety, inhibited Aβ42 aggregation through the autoxidation, followed by the Michael addition of Lys residues to oxidized (+)-taxifolin. In this Chapter, the author analyzed interaction sites between Aβ42 and (+)-taxifolin using solid-state NMR, to discuss the inhibitory mechanism by the non-catechol-type flavonoids.

## Result and discussion

The B-ring of (+)-taxifolin was labeled with $^{13}C_6$ based on the structure-activity relationship studies (Fig. 9); the catechol moiety on the B-ring is critical in the inhibitory potential, while the methylation of hydroxyl group at position 7 on the A-ring is less. Aβ42 was also $^{13}C$-labeled site-specifically at Ala2, Ser8, Lys16, Val18, Phe19, and Phe20, in which only $C_\beta$ in Phe19 and Phe20 was labeled to avoid the overlapping of the signals of Aβ42 and (+)-taxifolin. The $^{13}C$ chemical shifts of labeled Aβ42 and (+)-taxifolin were assigned according to 1D-$^{13}C$ cross polarization/magic angle spinning (CP/MAS) NMR and two dimensional-dipolar-assisted

rotational resonance (2D-DARR) spectra with 50 ms of mixing time (Figs. 19 and 20B).

DARR was employed for the broadband $^{13}C$-$^{13}C$ correlation 2D experiments.[117,118] In general, when the mixing time is 50 ms, cross peaks of carbon atoms mean that the distance between these atoms is 1.5-3 Å. On the other hand, when the mixing time is 500 ms, cross peaks of carbon atoms within 5-6 Å will be observed. However, the cross peaks between Aβ42 and (+)-taxifolin at mixing time of 500 ms were as weak as noise signals despite of the use of a ten-fold excess of (+)-taxifolin [Aβ42 : (+)-taxifolin = 13 : 145 μM, Fig. 20B], while a five-fold excess was employed for curcumin (Aβ42 : curcumin = 10 : 50 μM, Fig. 20A).[69] More specifically, the $^{13}C$-$^{13}C$ cross peaks between Lys residues and B-ring of (+)-taxifolin was not significantly obtained (Fig. 20B). The interaction of (+)-taxifolin with the aromatic hydrophobic core (Aβ17-21), which was seen in the curcumin experiment due to its inherent hydrophobicity and planarity,[69] was also not observed. These results indicate that the inhibitory mechanism of Aβ42 aggregation by (+)-taxifolin (*via* covalent bonding) might be different from that of curcumin (*via* intercalation).

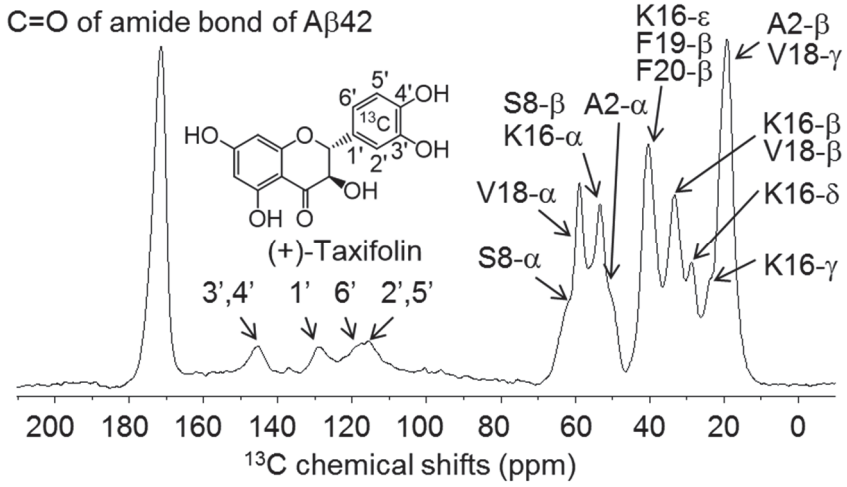


**Figure 19** 1D-$^{13}C$ CP/MAS NMR spectra of Aβ42 and (+)-taxifolin.

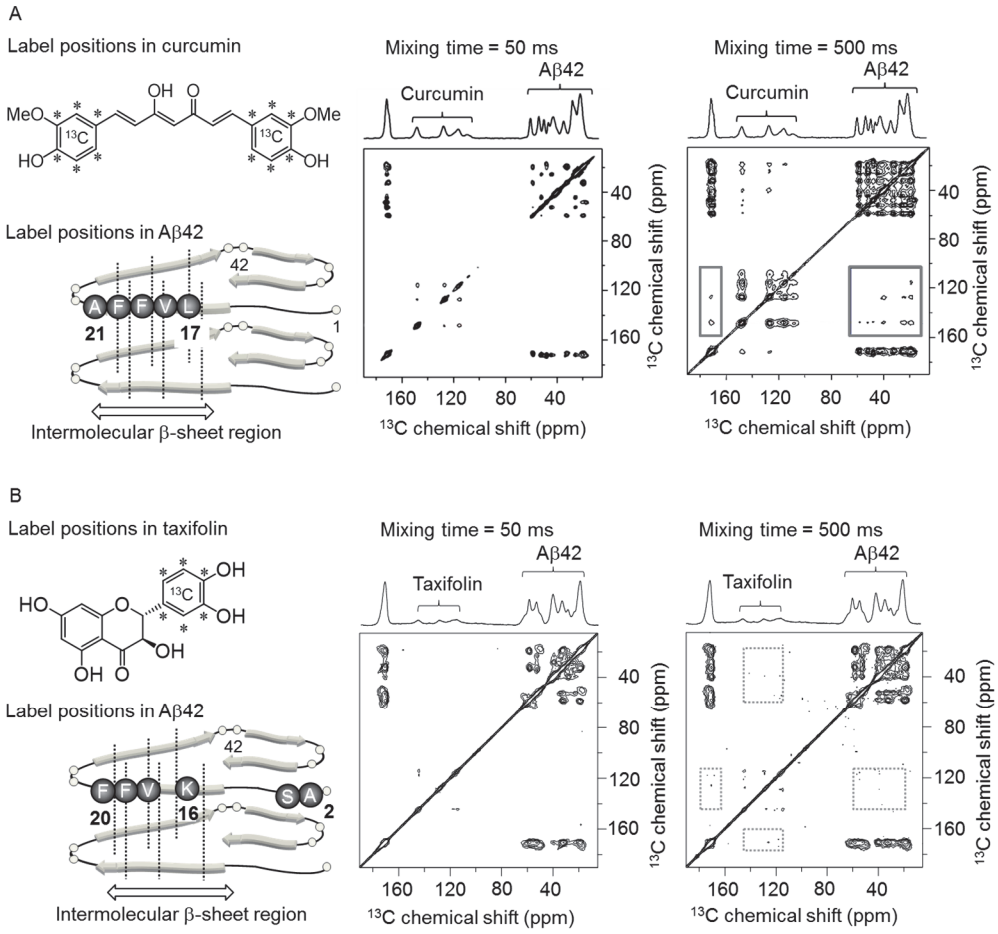


**Figure 20** 2D covariance DAAR spectra of (A) curcumin or (B) (+)-taxifolin and labeled Aβ42. In the spectra at mixing time of 500 ms, the intermolecular cross peaks (A, gray solid square) between Aβ42 and curcumin were detected, whereas those (B, gray dashed square) between Aβ42 and (+)-taxifolin were not. In the spectra at mixing time of 50 ms, no cross peaks in both the cases were found.

Since lack of the double bond at positions 2 and 3 of (+)-taxifolin could decreases its planarity, it might not be able to insert into the β-sheet region of the Aβ42 aggregate (Lys16~Ala21). Instability of the oxidized taxifolin–Aβ42 adduct might be another reason. The previous solution-state NMR studies on myricetin and Aβ42[72] suggested the less-specific broad recognition of the β-sheet region, possibly due to the usage of excessive amounts of myricetin (Aβ42 : myricetin = 25 : 200 μM). These findings might reflect the difference in the suppressive ability between myricetin and (+)-taxifolin against K16Nle-Aβ42 (Fig. 17A).

As shown in Chapter 3, the molecular recognition of non-catechol-type compounds with an α,β-unsaturated ketone (morin, kaempferol, and datiscetin) to Aβ42 could be different from that of (+)-taxifolin (Figs. 16 and 17). Because the carbon-carbon double bond on the C-ring can help let one hydroxyl group on the B-ring conjugate with an α,β-unsaturated ketone moiety to form the planar configuration, it is plausible that these non-catechol flavonols might intercalate the intermolecular β-sheet of the Aβ42 aggregate *via* π-π stacking, in a similar manner to curcumin.[69] The inability of galangin to prevent the aggregation of Aβ42 might be due to the lack of the hydroxyl group on the B-ring that might be involved in the hydrogen bonding with some residues in Aβ42. This strongly suggests the planarity of flavonoids not to be the primary feature to preventing Aβ42 aggregation. The planarity on the A-ring might collaterally participate in the inhibition *via* the hydrophobic interaction with the hydrophobic residues of Aβ42. Indeed, the importance of a hydroxyl group has also been documented in the interaction between curcumin and Aβ42.[69]

## Experimental procedures

*Fmoc protection of labeled amino acid*

L-Alanine ($^{13}C_3$, $^{15}N$), L-phenylalanine ($^{13}C_\beta$), and L-valine ($^{13}C_5$, $^{15}N$) were purchased from Isotec (Miamisburg, OH), and L-lysine ($^{13}C_6$, $^{15}N_2$) and L-serine ($^{13}C_3$, $^{15}N$) from Cambridge Isotope Laboratories (Frontage Road Andover, MA). Each labeled amino acid was protected by an Fmoc group, as previously reported.[119,120] The structure of each Fmoc derivative was confirmed by $^1$H NMR, $^{13}$C NMR, and FAB-MS.

*Synthesis of labeled Aβ42*

$^{13}$C, $^{15}$N-labeled Aβ42 was synthesized in the same manner as described in Chapter 2. The molecular weight of labeled Aβ42 was confirmed by MALDI-TOF-MS (AXIMA-CFR); A2, S8, K16, V18-$^{13}$C, $^{15}$N-uniformally, F19 and F20-$^{13}C_\beta$-labeled Aβ42 (*m/z*, calcd: 4538.90, found: 4538.94 $[M+H]^+$).

*Synthesis of $^{13}C_6$-(+)-taxifolin*

$^{13}C_6$-(+)-Taxifolin was synthesized in a similar manner, as described in Chapter 2, using vanillin-ring-$^{13}C_6$ (Isotec) as a starting material (Scheme 1B). The structure was confirmed by using $^1$H NMR,[79] $^{13}$C NMR,[121] and EI-MS: $^1$H NMR (500 MHz, 295.2 K, acetone-$d_6$, 7.7 mM) δ 4.61 (1H, dd, $J$ = 11.5, 3.0 Hz), 5.01 (1H, dq, $J$ = 11.5, 4.0 Hz), 5.95 (1H, d, $J$ = 2.4 Hz), 5.99 (1H, d, $J$ = 2.4 Hz), 6.89 (1H, dm, $J$ = 157.0 Hz), 7.07 (1H, d, $J$ = 157.0 Hz), 11.7 (1H, brs). $^{13}$C NMR (125 MHz, 296.2 K, acetone-$d_6$, 7.7 mM) δ 73.2, 84.7, 96.1, 97.2, 101.5, 115.2-116.5 (m), 120.3-121.3 (m), 129.3-130.3 (m), 145.1-147.3 (m), 164.2, 165.1, 168.2, 198.0. EI-MS: *m/z*, calcd: 310, found: 310 $[M]^+$.

*Solid-state NMR analysis*

The labeled Aβ42 (13 μM) was incubated with $^{13}C_6$-(+)-taxifolin (145 μM) in PBS (50 mM sodium phosphate and 100 mM NaCl, pH 7.4) at 37 °C. After 48 h of incubation, the solution was centrifuged (27,720 *g*, PRP-20-2; Hitachi) for 15 min at 4 °C, and then the precipitate was dried *in vacuo* to give the labeled Aβ42 aggregate associated with $^{13}C_6$-(+)-taxifolin (12 mg). The solid-state NMR experiments were performed at 14 T (600 MHz for $^1$H) using a JEOL ECA-600 spectrometer and a custom-fabricated probe with a Chemagnetics 3.2 mm spinning system at a magic angle spinning (MAS) frequency of 21 kHz at room temperature as reported previously.[69] The $^{13}$C chemical shifts were calibrated in ppm relative to tetramethylsilane by considering the $^{13}$C chemical shift for methine $^{13}$C of solid adamantine (29.5 ppm) as an external reference. For the broadband $^{13}$C-$^{13}$C correlation 2D experiments, DARR was used.[118] Pulse sequence parameters of the NMR experiment were as follows; two pulse phase-modulated (TPPM) $^1$H decoupling power = 80 kHz, ramped-amplitude cross polarization (RAMP-CP) contact time = 1.2 ms, pulse delay = 2 s, $t_1$ increment = 23.7 μs, $t_1$ points of 2D = 128 pt, and mixing time (τm) = 50 ms or 500 ms. The window function

'HAMMING' was used in all 2D FT spectra to minimize $t_1$ noise. As the 2D FT DARR spectra were difficult to analyze because of the $t_1$ noise (data not shown), covariance data processing was applied to obtain a better representation of the 2D spectrum (Fig. 20). After Fourier transformation along the $t2$ dimension and phase correction, the resulting data matrix was used for covariance processing as previously reported.[122] The covariance processing step was accelerated by singular value decomposition.[123]

# Summary and conclusion

Alzheimer's disease (AD) is characterized by the deposition of 40- and 42-mer amyloid β-proteins (Aβ40 and Aβ42) in the brain.[5,6] These proteins mainly aggregate through the formation of intermolecular β-sheets and exhibit neurotoxicity. Aβ42 plays a more critical role in the pathogenesis of AD than Aβ40 because of its higher aggregative ability and neurotoxicity.[4] Anti-aggregative agents for Aβ42 may be promising AD therapeutics because the deposition of Aβ has been detected 15 years before the onset of symptoms, followed by increase in tau protein levels in the CSF, hippocampal atrophy, and declines in cognitive and clinical function.[2]

The findings of a previous study by Murata *et al.*[76] demonstrated that silymarin, a methanol extract from *Silybum marianum*, suppressed Aβ fibril formation and neurotoxicity in PC12 cells *in vitro*. Furthermore, the oral administration of silymarin to an AD mouse model (J20 line) reduced several AD-like pathologies induced from Aβ aggregation, but not from the production of Aβ. Therefore, the protective effect of silymarin on AD pathogenesis may be attributed to the inhibition of Aβ aggregation.

In this research, (+)-taxifolin was identified as one of the active components with anti-aggregative ability against Aβ42 among six flavonoids isolated from silymarin (Fig. 8). Structure-activity relationship studies using the methylated derivatives of (+)-taxifolin and its enantiomer, (–)-taxifolin, clarified the significance of the catechol moiety on the B-ring of (+)-taxifolin in the anti-aggregative properties of Aβ42 (Fig. 9A, B). The addition of $NaIO_4$, an oxidant, accelerated the inhibitory ability of (+)-taxifolin, while it did not prevent Aβ42 aggregation under anaerobic conditions or in the presence of TCEP, a reductant (Figs. 11 and 12). These results strongly suggest the involvement of (+)-taxifolin autoxidation, which forms the *o*-quinone structure, in preventing Aβ42 aggregation.

The mechanism underlying Aβ42 aggregation, which is composed of two steps, a nucleation phase and extension phase, is known as a nucleation-dependent polymerization model.[11,12] (+)-Taxifolin inhibited the extension phase of Aβ42 in the presence of the Aβ42 seed (nuclear), rather than the nucleation phase (Fig. 11), which indicated that the autoxidation of (+)-taxifolin could require more time in the nucleation phase (~1 h) based on

the results obtained from UV measurements (Fig. 12).

Because the Michael addition of the basic amino acid residues (Arg5, Lys16 or Lys28) of Aβ42 with the *o*-quinone structure in oxidized (+)-taxifolin was observed using LC-MS analysis (Fig. 14), the anti-aggregative ability of (+)-taxifolin was estimated against Aβ42 mutants, in which basic amino acid residues were substituted with norleucine (Nle), in order to identify which amino acid residues were involved. (+)-Taxifolin did not suppress the aggregation of Aβ42 mutants at Lys16 and/or Lys28, except for the mutant at Arg5. The aggregation of Aβ42 was also prevented by other catechol-type flavonoids, while that of K16Nle-Aβ42 was not. These results indicate that the formation of covalent bonding with Lys residues (especially Lys16) is essential for the inhibition of Aβ42 aggregation by the catechol-type flavonoids (Figs. 15 and 18).

In contrast, some non-catechol-type flavonoids (morin, datiscetin, and kampferol) prevented Aβ42 aggregation even under anaerobic conditions. In addition, the aggregation of K16Nle-Aβ42 as well as Aβ42 was suppressed by these compounds. These results imply the existence of another inhibitory mechanism for non-catechol-type flavonoids. Solid-state NMR studies proposed that the inhibitory mechanism for Aβ42 aggregation by (+)-taxifolin was different from that of curcumin, a representative non-catechol-type polyphenol with anti-aggregative ability, which interacted with the β-sheet region in Aβ42 aggregates through π/π stacking and hydrophobicity (Fig. 20).

These findings may provide a new strategy for the design and development of aggregation inhibitors to be used in the treatment of AD.

# Acknowledgement

This study was conducted in the Laboratory of Organic Chemistry in Life Science, Division of Food Science and Biotechnology, Graduate School of Agriculture, Kyoto University, between 2010 and 2013.

The author would like to express her sincere thanks to Dr. Kazuhiro Irie, Professor of Kyoto University, for his insightful propositions, thoughtful encouragement, and continuous guidance. The author would like to offer her special thanks to Dr. Kazuma Murakami, Associate Professor of Kyoto University, for his practical suggestions, constructive guidance, warm encouragement, and extensive discussions. This study could not have been completed without their guidance. The author also expresses her deepest appreciation to Dr. Nobuhiro Hirai, Professor of Kyoto University, and Dr. Akira Murakami, Assistant Professor of Kyoto University, for their insightful suggestions and continuous encouragement.

The author is grateful to Dr. Kenichi Akagi and Dr. Sumie Katayama at the National Institute of Biomedical Innovation for their assistance with electron microscopy, valuable comments, and constant help. The author thanks to Dr. Yuichi Masuda, Assistant Professor of Tohoku University and Dr. Kiyonori Takegoshi, Professor of Kyoto University, for assisting with solid-state NMR measurements, tremendous support, and beneficial suggestions. The author also thanks Dr. Yu Nakagawa at the RIKEN Advanced Science Institute, for his incisive advice, and Dr. Nobutaka Fujii, Professor of Kyoto University and Dr. Shinya Oishi, Lecturer of Kyoto University, for their permission to use MALDI-TOF-MS and LC-MS. The author feels gratitude to Ms. Mayumi Okano-Uno and Ms. Haruko Ikubo of Kyoto University for their significant contributions, and to all members of the Laboratory of Organic Chemistry in Life Science for their considerable encouragement. The author expresses her heartfelt gratitude to Dr. Naomichi Baba, Emeritus Professor of Okayama University, Dr. Shuhei Nakajima, Professor of Okayama University, and Dr. Minoru Izumi, Associate Professor of Okayama University for their thoughtful guidance and continued encouragement at Okayama University.

This research was supported in part by a Grant-in-aid for the Promotion

of Science for Young Scientists Grant from The Ministry of Education, Culture, Sports, Science and Technology, Japan.

Finally, the author would like to express her deepest respect and gratitude to her family, Yasuhiko Sato, Setsuko Sato, Ayako Ito, Mitsuhiro Sato, and Masako Maeda for their understanding, continuing support, sincere encouragement, and endless love during her long-term study.

# References


1. Babusikova, E., Evinova, A., Jurecekova, J., Jesenak, M., and Dobrota, D. (2011) Alzheimer's disease: definition, molecular and genetic factors, advanced understanding of neurodegenerative diseases. ISBN: 978-953-307-529-7, InTech, DOI: 10.5772/29027.
2. Bateman, R. J., Xiong, C., Benzinger, T. L. S., Fagan, A. M., Goate, A., Fox, N. C., Marcus, D. S., Cairns, N. J., Xie, X., Blazey, T. M., Holtzman, D. M., Santacruz, A., Buckles, V., Oliver, A., Moulder, K., Aisen, P. S., Ghetti, B., Klunk, W. E., McDade, E., Martins, R. N., Masters, C. L., Mayeux, R., Ringman, J. M., Rossor, M. N., Schofield, P. R., Sperling, R. A., Salloway, S., and Morris, J. C. (2012) Clinical and biomarker changes in dominantly inherited Alzheimer's disease. *N. Engl. J. Med.* **367**, 795-804
3. Reitz, C. (2012) Alzheimer's disease and the amyloid cascade hypothesis: a critical review. *Int. J. Alzheimers Dis.* **2012**, 369808
4. Haass, C., and Selkoe, D. J. (2007) Soluble protein oligomers in neurodegeneration: lessons from the Alzheimer's amyloid β-peptide. *Nat. Rev. Mol. Cell Biol.* **8**, 101-112
5. Glenner, G. G., and Wong, C. W. (1984) Alzheimer's disease: initial report of the purification and characterization of a novel cerebrovascular amyloid protein. *Biochem. Biophys. Res. Commun.* **120**, 885-890
6. Masters, C. L., Simms, G., Weinman, N. A., Multhaup, G., McDonald, B. L., and Beyreuther, K. (1985) Amyloid plaque core protein in Alzheimer disease and Down syndrome. *Proc. Natl. Acad. Sci. USA* **82**, 4245-4249
7. Haass, C. (2004) Take five—BACE and the γ-secretase quartet conduct Alzheimer's amyloid β-peptide generation. *EMBO J.* **23**, 483-488
8. Saito, T., Suemoto, T., Brouwers, N., Sleegers, K., Funamoto, S., Mihira, N., Matsuba, Y., Yamada, K., Nilsson, P., Takano, J., Nishimura, M., Iwata, N., Van Broeckhoven, C., Ihara, Y., and Saido, T. C. (2011) Potent amyloidogenicity and pathogenicity of Aβ43. *Nat. Neurosci.* **14**, 1023-1032
9. Zheng, H., and Koo, E. (2011) Biology and pathophysiology of the amyloid precursor protein. *Mol. Neurodegener.* **6**, 27
10. Tanzi, R. E. (2012) The genetics of Alzheimer disease. *Cold Spring Harb. Perspect. Med.* **2**, DOI: 10.1101/cshperspect.a006296
11. Hasegawa, K., Yamaguchi, I., Omata, S., Gejyo, F., and Naiki, H. (1999) Interaction between Aβ(1−42) and Aβ(1−40) in Alzheimer's β-amyloid fibril formation in vitro. *Biochemistry* **38**, 15514-15521
12. Ono, K., Hamaguchi, T., Naiki, H., and Yamada, M. (2006) Anti-amyloidogenic effects of antioxidants: implications for the prevention and therapeutics of Alzheimer's disease. *Biochim. Biophys. Acta* **1762**, 575-586

13. Roychaudhuri, R., Yang, M., Hoshi, M. M., and Teplow, D. B. (2009) Amyloid β-protein assembly and Alzheimer disease. *J. Biol. Chem.* **284**, 4749-4753
14. Hardy, J., and Allsop, D. (1991) Amyloid deposition as the central event in the aetiology of Alzheimer's disease. *Trends Pharmacol. Sci.* **12**, 383-388
15. Walsh, D. M., Klyubin, I., Fadeeva, J. V., Cullen, W. K., Anwyl, R., Wolfe, M. S., Rowan, M. J., and Selkoe, D. J. (2002) Naturally secreted oligomers of amyloid β protein potently inhibit hippocampal long-term potentiation *in vivo*. *Nature* **416**, 535-539
16. Shankar, G. M., Li, S., Mehta, T. H., Garcia-Munoz, A., Shepardson, N. E., Smith, I., Brett, F. M., Farrell, M. A., Rowan, M. J., Lemere, C. A., Regan, C. M., Walsh, D. M., Sabatini, B. L., and Selkoe, D. J. (2008) Amyloid-β protein dimers isolated directly from Alzheimer's brains impair synaptic plasticity and memory. *Nat. Med.* **14**, 837-842
17. Benilova, I., Karran, E., and De Strooper, B. (2012) The toxic Aβ oligomer and Alzheimer's disease: an emperor in need of clothes. *Nat. Neurosci.* **15**, 349-357
18. Verdier, Y., Zarándi, M., and Penke, B. (2004) Amyloid β-peptide interactions with neuronal and glial cell plasma membrane: binding sites and implications for Alzheimer's disease. *J. Pept. Sci.* **10**, 229-248
19. Sayre, L. M., Perry, G., and Smith, M. A. (2007) Oxidative stress and neurotoxicity. *Chem. Res. Toxicol.* **21**, 172-188
20. Butterfield, D. A., Reed, T., Newman, S. F., and Sultana, R. (2007) Roles of amyloid β-peptide-associated oxidative stress and brain protein modifications in the pathogenesis of Alzheimer's disease and mild cognitive impairment. *Free Radic. Biol. Med.* **43**, 658-677
21. Varadarajan, S., Yatin, S., Aksenova, M., and Butterfield, D. A. (2000) Review: Alzheimer's amyloid β-peptide-associated free radical oxidative stress and neurotoxicity. *J. Struct. Biol.* **130**, 184-208
22. Murakami, K., Irie, K., Ohigashi, H., Hara, H., Nagao, M., Shimizu, T., and Shirasawa, T. (2005) Formation and stabilization model of the 42-mer Aβ radical: implications for the long-lasting oxidative stress in Alzheimer's disease. *J. Am. Chem. Soc.* **127**, 15168-15174
23. Li, F., Calingasan, N. Y., Yu, F., Mauck, W. M., Toidze, M., Almeida, C. G., Takahashi, R. H., Carlson, G. A., Flint Beal, M., Lin, M. T., and Gouras, G. K. (2004) Increased plaque burden in brains of APP mutant MnSOD heterozygous knockout mice. *J. Neurochem.* **89**, 1308-1312
24. Murakami, K., Murata, N., Noda, Y., Tahara, S., Kaneko, T., Kinoshita, N., Hatsuta, H., Murayama, S., Barnham, K. J., Irie, K., Shirasawa, T., and Shimizu, T. (2011) SOD1 (Copper/zinc superoxide dismutase) deficiency drives amyloid β protein oligomerization and memory loss in mouse model of Alzheimer disease. *J. Biol. Chem.* **286**, 44557-44568
25. Barnham, K. J., Masters, C. L., and Bush, A. I. (2004) Neurodegenerative diseases and oxidative stress. *Nat. Rev. Drug Discov.* **3**, 205-214

26. Curtain, C. C., Ali, F., Volitakis, I., Cherny, R. A., Norton, R. S., Beyreuther, K., Barrow, C. J., Masters, C. L., Bush, A. I., and Barnham, K. J. (2001) Alzheimer's disease amyloid-β binds copper and zinc to generate an allosterically ordered membrane-penetrating structure containing superoxide dismutase-like subunits. *J. Biol. Chem.* **276**, 20466-20473
27. Sarell, C. J., Syme, C. D., Rigby, S. E. J., and Viles, J. H. (2009) Copper(II) binding to amyloid-β fibrils of Alzheimer's disease reveals a picomolar affinity: stoichiometry and coordination geometry are independent of Aβ oligomeric form. *Biochemistry* **48**, 4388-4402
28. Huang, X., Cuajungco, M. P., Atwood, C. S., Hartshorn, M. A., Tyndall, J. D. A., Hanson, G. R., Stokes, K. C., Leopold, M., Multhaup, G., Goldstein, L. E., Scarpa, R. C., Saunders, A. J., Lim, J., Moir, R. D., Glabe, C., Bowden, E. F., Masters, C. L., Fairlie, D. P., Tanzi, R. E., and Bush, A. I. (1999) Cu(II) Potentiation of Alzheimer Aβ neurotoxicity: corrlation sith cell-frer hydrogen peroxide production and metal reduction. *J. Biol. Chem.* **274**, 37111-37116
29. Smith, D. G., Cappai, R., and Barnham, K. J. (2007) The redox chemistry of the Alzheimer's disease amyloid β peptide. *Biochim. Biophys. Acta* **1768**, 1976-1990
30. Naslund, J., Schierhorn, A., Hellman, U., Lannfelt, L., Roses, A. D., Tjernberg, L. O., Silberring, J., Gandy, S. E., Winblad, B., and Greengard, P. (1994) Relative abundance of Alzheimer Aβ amyloid peptide variants in Alzheimer disease and normal aging. *Proc. Natl. Acad. Sci. USA* **91**, 8378-8382
31. Butterfield, D. A. (2003) Amyloid β-peptide [1-42]-associated free radical-induced oxidative stress and neurodegeneration in Alzheimer's disease brain: mechanisms and consequences. *Curr. Med. Chem.* **10**, 2651-2659
32. Pal, R., Oien, D., Ersen, F., and Moskovitz, J. (2007) Elevated levels of brain-pathologies associated with neurodegenerative diseases in the methionine sulfoxide reductase a knockout mouse. *Exp. Brain Res.* **180**, 765-774
33. Grill, J. D., and Cummings, J. L. (2010) Current therapeutic targets for the treatment of Alzheimer's disease. *Expert Rev. Neurother.* **10**, 711-728
34. Aderinwale, O. G., Ernst, H. W., and Mousa, S. A. (2010) Current therapies and new strategies for the management of Alzheimer's disease. *Am. J. Alzheimers Dis. Other Demen.* **25**, 414-424
35. Cacabelos, R. (2007) Donepezil in Alzheimer's disease: from conventional trials to pharmacogenetics. *Neuropsychiatr. Dis. Treat.* **3**, 303-333
36. Smid, S. D., Maag, J. L., and Musgrave, I. F. (2012) Dietary polyphenol-derived protection against neurotoxic β-amyloid protein: from molecular to clinical. *Food Funct.* **3**, 1242-1250
37. Barten, D., and Albright, C. (2008) Therapeutic strategies for Alzheimer's disease. *Mol. Neurobiol.* **37**, 171-186

38. Citron, M. (2010) Alzheimer's disease: strategies for disease modification. *Nat. Rev. Drug. Discov.* **9**, 387-398
39. McLaurin, J., Golomb, R., Jurewicz, A., Antel, J. P., and Fraser, P. E. (2000) Inositol stereoisomers stabilize an oligomeric aggregate of Alzheimer amyloid β peptide and inhibit Aβ-induced toxicity. *J. Biol. Chem.* **275**, 18495-18502
40. McLaurin, J., Kierstead, M. E., Brown, M. E., Hawkes, C. A., Lambermon, M. H. L., Phinney, A. L., Darabie, A. A., Cousins, J. E., French, J. E., Lan, M. F., Chen, F., Wong, S. S. N., Mount, H. T. J., Fraser, P. E., Westaway, D., and George-Hyslop, P. S. (2006) Cyclohexanehexol inhibitors of Aβ aggregation prevent and reverse Alzheimer phenotype in a mouse model. *Nat. Med.* **12**, 801-808
41. Fenili, D., Brown, M., Rappaport, R., and McLaurin, J. (2007) Properties of *scyllo*–inositol as a therapeutic treatment of AD-like pathology. *J. Mol. Med.* **85**, 603-611
42. Fokkens, M., Schrader, T., and Klärner, F.-G. (2005) A molecular tweezer for lysine and arginine. *J. Am. Chem. Soc.* **127**, 14415-14421
43. Sinha, S., Lopes, D. H. J., Du, Z., Pang, E. S., Shanmugam, A., Lomakin, A., Talbiersky, P., Tennstaedt, A., McDaniel, K., Bakshi, R., Kuo, P., Ehrmann, M., Benedek, G. B., Loo, J. A., Klärner, F.-G., Schrader, T., Wang, C., and Bitan, G. (2011) Lysine-specific molecular tweezers are broad-spectrum inhibitors of assembly and toxicity of amyloid proteins. *J. Am. Chem. Soc.* **133**, 16958-16969
44. Attar, A., Ripoli, C., Riccardi, E., Maiti, P., Li Puma, D. D., Liu, T., Hayes, J., Jones, M. R., Lichti-Kaiser, K., Yang, F., Gale, G. D., Tseng, C. H., Tan, M., Xie, C. W., Straudinger, J. L., Klarner, F. G., Schrader, T., Frautschy, S. A., Grassi, C., and Bitan, G. (2012) Protection of primary neurons and mouse brain from Alzheimer's pathology by molecular tweezers. *Brain* **135**, 3735-3748
45. Adlard, P. A., Cherny, R. A., Finkelstein, D. I., Gautier, E., Robb, E., Cortes, M., Volitakis, I., Liu, X., Smith, J. P., Perez, K., Laughton, K., Li, Q., Charman, S. A., Nicolazzo, J. A., Wilkins, S., Deleva, K., Lynch, T., Kok, G., Ritchie, C. W., Tanzi, R. E., Cappai, R., Masters, C. L., Barnham, K. J., and Bush, A. I. (2008) Rapid restoration of cognition in Alzheimer's transgenic mice with 8-hydroxy quinoline analogs is associated with decreased interstitial Aβ. *Neuron* **59**, 43-55
46. Lannfelt, L., Blennow, K., Zetterberg, H., Batsman, S., Ames, D., Harrison, J., Masters, C. L., Targum, S., Bush, A. I., Murdoch, R., Wilson, J., and Ritchie, C. W. (2008) Safety, efficacy, and biomarker findings of PBT2 in targeting Aβ as a modifying therapy for Alzheimer's disease: a phase IIa, double-blind, randomised, placebo-controlled trial. *Lancet Neurol.* **7**, 779-786
47. Mecocci, P., and Polidori, M. C. (2012) Antioxidant clinical trials in mild cognitive impairment and Alzheimer's disease. *Biochim. Biophys. Acta* **1822**, 631-638

48. Ramassamy, C. (2006) Emerging role of polyphenolic compounds in the treatment of neurodegenerative diseases: a review of their intracellular targets. *Eur. J. Pharmacol.* **545**, 51-64
49. Porat, Y., Abramowitz, A., and Gazit, E. (2006) Inhibition of amyloid fibril formation by polyphenols: structural similarity and aromatic interactions as a common inhibition mechanism. *Chem. Biol. Drug Des.* **67**, 27-37
50. Rossi, L., Mazzitelli, S., Arciello, M., Capo, C. R., and Rotilio, G. (2008) Benefits from dietary polyphenols for brain aging and Alzheimer's disease. *Neurochem. Res.* **33**, 2390-2400
51. Williams, R. J., and Spencer, J. P. E. (2012) Flavonoids, cognition, and dementia: actions, mechanisms, and potential therapeutic utility for Alzheimer disease. *Free Radic. Biol. Med.* **52**, 35-45
52. Ganguli, M., Dodge, H. H., Chen, P., Belle, S., and DeKosky, S. T. (2000) Ten-year incidence of dementia in a rural elderly US community population: the MoVIES project. *Neurology* **54**, 1109-1116
53. Palanivelu, K., and Mishra, S. (2008) The effect of curcumin (turmeric) on Alzheimer's disease : an overview. *Ann. Indian Acad. Neurol.* **11**, 13-19
54. Ono, K., Hasegawa, K., Naiki, H., and Yamada, M. (2004) Curcumin has potent anti-amyloidogenic effects for Alzheimer's β-amyloid fibrils in vitro. *J. Neurosci. Res.* **75**, 742-750
55. Garcia-Alloza, M., Borrelli, L. A., Rozkalne, A., Hyman, B. T., and Bacskai, B. J. (2007) Curcumin labels amyloid pathology in vivo, disrupts existing plaques, and partially restores distorted neurites in an Alzheimer mouse model. *J. Neurochem.* **102**, 1095-1104
56. Kim, D. S. H. L., Park, S., and Kim, J. (2001) Curcuminoids from *Curcuma longa L.* (Zingiberaceae) that protect PC12 rat pheochromocytoma and normal human umbilical vein endothelial cells from βA(1–42) insult. *Neurosci. Lett.* **303**, 57-61
57. Reinke, A. A., and Gestwicki, J. E. (2007) Structure–activity relationships of amyloid beta-aggregation inhibitors based on curcumin: influence of linker length and flexibility. *Chem. Biol. Drug Des.* **70**, 206-215
58. Truelsen, T., Thudium, D., and Gronbaek, M. (2002) Amount and type of alcohol and risk of dementia: the copenhagen city heart study. *Neurology* **59**, 1313-1319
59. Ladiwala, A. R. A., Lin, J. C., Bale, S. S., Marcelino-Cruz, A. M., Bhattacharya, M., Dordick, J. S., and Tessier, P. M. (2010) Resveratrol selectively remodels soluble oligomers and fibrils of amyloid Aβ into off-pathway conformers. *J. Biol. Chem.* **285**, 24228-24237
60. Feng, Y., Wang, X., Yang, S., Wang, Y., Zhang, X., Du, X., Sun, X., Zhao, M., Huang, L., and Liu, R. (2009) Resveratrol inhibits beta-amyloid oligomeric cytotoxicity but does not prevent oligomer formation. *Neurotoxicology* **30**, 986-995
61. Li, F., Gong, Q., Dong, H., and Shi, J. (2012) Reveratrol, a

neuroprotective supplement for Alzheimer's disease. *Curr. Pharm. Des.* **18**, 27-33
62. Ehrnhoefer, D. E., Bieschke, J., Boeddrich, A., Herbst, M., Masino, L., Lurz, R., Engemann, S., Pastore, A., and Wanker, E. E. (2008) EGCG redirects amyloidogenic polypeptides into unstructured, off-pathway oligomers. *Nat. Struct. Mol. Biol.* **15**, 558-566
63. Choi, Y., Jung, C., Lee, S., Bae, J., Baek, W., Suh, M., Park, J., Park, C., and Suh, S. (2001) The green tea polyphenol (−)-epigallocatechin gallate attenuates β-amyloid-induced neurotoxicity in cultured hippocampal neurons. *Life Sci.* **70**, 603-614
64. Rezai-Zadeh, K., Arendash, G. W., Hou, H., Fernandez, F., Jensen, M., Runfeldt, M., Shytle, R. D., and Tan, J. (2008) Green tea epigallocatechin-3-gallate (EGCG) reduces β-amyloid mediated cognitive impairment and modulates tau pathology in Alzheimer transgenic mice. *Brain Res.* **1214**, 177-187
65. Ushikubo, H., Watanabe, S., Tanimoto, Y., Abe, K., Hiza, A., Ogawa, T., Asakawa, T., Kan, T., and Akaishi, T. (2012) 3,3',4',5,5'-Pentahydroxyflavone is a potent inhibitor of amyloid β fibril formation. *Neurosci. Lett.* **513**, 51-56
66. Gravitz, L. (2011) Drugs: a tangled web of targets. *Nature* **475**, S9-S11
67. Baum, L., Lam, C. W., Cheung, S. K., Kwok, T., Lui, V., Tsoh, J., Lam, L., Leung, V., Hui, E., Ng, C., Woo, J., Chiu, H. F., Goggins, W. B., Zee, B. C., Cheng, K. F., Fong, C. Y., Wong, A., Mok, H., Chow, M. S., Ho, P. C., Ip, S. P., Ho, C. S., Yu, X. W., Lai, C. Y., Chan, M. H., Szeto, S., Chan, I. H., and Mok, V. (2008) Six-month randomized, placebo-controlled, double-blind, pilot clinical trial of curcumin in patients with Alzheimer disease. *J. Cli. Psychopharmacol.* **28**, 110-113
68. Keshet, B., Gray, J. J., and Good, T. A. (2010) Structurally distinct toxicity inhibitors bind at common loci on β-amyloid fibril. *Protein Sci.* **19**, 2291-2304
69. Masuda, Y., Fukuchi, M., Yatagawa, T., Tada, M., Takeda, K., Irie, K., Akagi, K., Monobe, Y., Imazawa, T., and Takegoshi, K. (2011) Solid-state NMR analysis of interaction sites of curcumin and 42-residue amyloid β-protein fibrils. *Bioorg. Med. Chem.* **19**, 5967-5974
70. Lopez del Amo, J. M., Fink, U., Dasari, M., Grelle, G., Wanker, E. E., Bieschke, J., and Reif, B. (2012) Structural properties of EGCG-induced, nontoxic Alzheimer's disease Aβ oligomers. *J. Mol. Biol.* **421**, 517-524
71. Sinha, S., Du, Z., Maiti, P., Klärner, F.-G., Schrader, T., Wang, C., and Bitan, G. (2012) Comparison of three amyloid assembly inhibitors: the sugar *scyllo*-inositol, the polyphenol epigallocatechin gallate, and the molecular tweezer CLR01. *ACS Chem. Neurosci.* **3**, 451-458
72. Ono, K., Li, L., Takamura, Y., Yoshiike, Y., Zhu, L., Han, F., Mao, X., Ikeda, T., Takasaki, J., Nishijo, H., Takashima, A., Teplow, D. B., Zagorski, M. G., and Yamada, M. (2012) Phenolic compounds prevent amyloid β-protein oligomerization and synaptic dysfunction by

site-specific binding. *J. Biol. Chem.* **287**, 14631-14643
73. Lee, J. I., Narayan, M., and Barrett, J. S. (2007) Analysis and comparison of active constituents in commercial standardized silymarin extracts by liquid chromatography–electrospray ionization mass spectrometry. *J. Chromatogr. B* **845**, 95-103
74. Morazzoni, P., Montalbetti, A., Malandrino, S., and Pifferi, G. (1993) Comparative pharmacokinetics of silipide and silymarin in rats. *Eur. J. Drug Metabol. Pharmacokinet.* **18**, 289-297
75. Valenzuela, A., Barría, T., Guerra, R., and Garrido, A. (1985) Inhibitory effect of the flavonoid silymarin on the erythrocyte hemolysis induced by phenylhydrazine. *Biochem. Biophys. Res. Commun.* **126**, 712-718
76. Murata, N., Murakami, K., Ozawa, Y., Kinoshita, N., Irie, K., Shirasawa, T., and Shimizu, T. (2010) Silymarin attenuated the amyloid β plaque burden and improved behavioral abnormalities in an Alzheimer's disease mouse model. *Biosci. Biotechnol. Biochem.* **74**, 2299-2306
77. Lee, D. Y. W., and Liu, Y. (2003) Molecular structure and stereochemistry of silybin A, silybin B, isosilybin A, and isosilybin B, isolated from *Silybum marianum* (Milk Thistle). *J. Nat. Prod.* **66**, 1171-1174
78. MacKinnon, S. L., Hodder, M., Craft, C., and Simmons-Boyce, J. (2007) Silyamandin, a new flavonolignan isolated from milk thistle tinctures. *Planta Med.* **73**, 1214-1216
79. Kiehlmann, E., and Slade, P. W. (2003) Methylation of dihydroquercetin acetates: synthesis of 5-*O*-methyldihydroquercetin. *J. Nat. Prod.* **66**, 1562-1566
80. Kim, N., Graf, T. N., Sparacino, C. M., Wani, M. C., and Wall, M. E. (2003) Complete isolation and characterization of silybins and isosilybins from milk thistle (*Silybum marianum*). *Org. Biomol. Chem.* **1**, 1684-1689
81. Tanaka, H., Hiroo, M., Ichino, K., and Ito, K. (1989) Total synthesis of silychristin, an antihepatotoxic flavonolignan. *Chem. Pharm. Bull.* **37**, 1441-1445
82. Murakami, K., Irie, K., Morimoto, A., Ohigashi, H., Shindo, M., Nagao, M., Shimizu, T., and Shirasawa, T. (2003) Neurotoxicity and physicochemical properties of Aβ mutant peptides from cerebral amyloid angiopathy. *J. Biol. Chem.* **278**, 46179-46187
83. Murakami, K., Irie, K., Morimoto, A., Ohigashi, H., Shindo, M., Nagao, M., Shimizu, T., and Shirasawa, T. (2002) Synthesis, aggregation, neurotoxicity, and secondary structure of various Aβ1–42 mutants of familial Alzheimer's disease at positions 21–23. *Biochem. Biophys. Res. Commun.* **294**, 5-10
84. Shearman, M. S., Ragan, C. I., and Iversen, L. L. (1994) Inhibition of PC12 cell redox activity is a specific, early indicator of the mechanism of β-amyloid-mediated cell death. *Proc. Natl. Acad. Sci. USA* **91**, 1470-1474
85. Roschek Jr, B., Fink, R. C., McMichael, M. D., Li, D., and Alberte, R. S. (2009) Elderberry flavonoids bind to and prevent H1N1 infection *in vitro*. *Phytochemistry* **70**, 1255-1261

86. Akaishi, T., Morimoto, T., Shibao, M., Watanabe, S., Sakai-Kato, K., Utsunomiya-Tate, N., and Abe, K. (2008) Structural requirements for the flavonoid fisetin in inhibiting fibril formation of amyloid β protein. *Neurosci. Lett.* **444**, 280-285
87. Ono, K., Yoshiike, Y., Takashima, A., Hasegawa, K., Naiki, H., and Yamada, M. (2003) Potent anti-amyloidogenic and fibril-destabilizing effects of polyphenols *in vitro*: implications for the prevention and therapeutics of Alzheimer's disease. *J. Neurochem.* **87**, 172-181
88. Borah, A., Paul, R., Choudhury, S., Choudhury, A., Bhuyan, B., Das Talukdar, A., Dutta Choudhury, M., and Mohanakumar, K. P. (2013) Neuroprotective potential of silymarin against CNS disorders: insight into the pathways and molecular mechanisms of action. *CNS Neurosci. Ther.* **19**, 847-853
89. Vega-Villa, K. R., Remsberg, C. M., Ohgami, Y., Yanez, J. A., Takemoto, J. K., Andrews, P. K., and Davies, N. M. (2009) Stereospecific high-performance liquid chromatography of taxifolin, applications in pharmacokinetics, and determination in tu fu ling (*Rhizoma smilacis glabrae*) and apple (*Malus x domestica*). *Biomed. Chromatogr.* **23**, 638-646
90. Irie, K., Oie, K., Nakahara, A., Yanai, Y., Ohigashi, H., Wender, P. A., Fukuda, H., Konishi, H., and Kikkawa, U. (1998) Molecular basis for protein kinase C isozyme-selective binding: the synthesis, folding, and phorbol ester binding of the cysteine-rich domeins of all protein kinase C isozymes. *J. Am. Chem. Soc.* **120**, 9159-9167
91. Naiki, H., and Gejyo, F. (1999) Kinetic analysis of amyloid fibril formation. *Methods Enzymol.* **309**, 305-318
92. Ishii, T., Mori, T., Tanaka, T., Mizuno, D., Yamaji, R., Kumazawa, S., Nakayama, T., and Akagawa, M. (2008) Covalent modification of proteins by green tea polyphenol (–)-epigallocatechin-3-gallate through autoxidation. *Free Radic. Biol. Med.* **45**, 1384-1394
93. Graham, D. G. (1978) Oxidative pathways for catecholamines in the genesis of neuromelanin and cytotoxic quinones. *Mol. Pharmacol.* **14**, 633-643
94. Graham, D. G., and Jeffs, P. W. (1977) The role of 2,4,5-trihydroxyphenylalanine in melanin biosynthesis. *J. Biol. Chem.* **252**, 5729-5734
95. Hou, L., Kang, I., Marchant, R. E., and Zagorski, M. G. (2002) Methionine 35 oxidation reduces fibril assembly of the amyloid Aβ-(1–42) peptide of Alzheimer's disease. *J. Biol. Chem.* **277**, 40173-40176
96. Kostyuk, V. A., Kraemer, T., Sies, H., and Schewe, T. (2003) Myeloperoxidase/nitrite-mediated lipid peroxidation of low-density lipoprotein as modulated by flavonoids. *FEBS Lett.* **537**, 146-150
97. Zhu, M., Rajamani, S., Kaylor, J., Han, S., Zhou, F., and Fink, A. L. (2004) The flavonoid baicalein inhibits fibrillation of α-synuclein and disaggregates existing fibrils. *J. Biol. Chem.* **279**, 26846-26857

98. Masuda, Y., Uemura, S., Ohashi, R., Nakanishi, A., Takegoshi, K., Shimizu, T., Shirasawa, T., and Irie, K. (2009) Identification of physiological and toxic conformations in Aβ42 aggregates. *ChemBioChem* **10**, 287-295
99. Morimoto, A., Irie, K., Murakami, K., Masuda, Y., Ohigashi, H., Nagao, M., Fukuda, H., Shimizu, T., and Shirasawa, T. (2004) Analysis of the secondary structure of β-amyloid (Aβ42) fibrils by systematic proline replacement. *J. Biol. Chem.* **279**, 52781-52788
100. Murakami, K., Horikoshi-Sakuraba, Y., Murata, N., Noda, Y., Masuda, Y., Kinoshita, N., Hatsuta, H., Murayama, S., Shirasawa, T., Shimizu, T., and Irie, K. (2010) Monoclonal antibody against the turn of the 42-residue amyloid β-Ppotein at positions 22 and 23. *ACS Chem. Neurosci.* **1**, 747-756
101. Kondo, T., Asai, M., Tsukita, K., Kutoku, Y., Ohsawa, Y., Sunada, Y., Imamura, K., Egawa, N., Yahata, N., Okita, K., Takahashi, K., Asaka, I., Aoi, T., Watanabe, A., Watanabe, K., Kadoya, C., Nakano, R., Watanabe, D., Maruyama, K., Hori, O., Hibino, S., Choshi, T., Nakahata, T., Hioki, H., Kaneko, T., Naitoh, M., Yoshikawa, K., Yamawaki, S., Suzuki, S., Hata, R., Ueno, S., Seki, T., Kobayashi, K., Toda, T., Murakami, K., Irie, K., Klein, W. L., Mori, H., Asada, T., Takahashi, R., Iwata, N., Yamanaka, S., and Inoue, H. (2013) Modeling Alzheimer's disease with iPSCs reveals stress phenotypes associated with intracellular Aβ and differential drug responsiveness. *Cell Stem Cell* **12**, 487-492
102. Kulic, L., McAfoose, J., Welt, T., Tackenberg, C., Spani, C., Wirth, F., Finder, V., Konietzko, U., Giese, M., Eckert, A., Noriaki, K., Shimizu, T., Murakami, K., Irie, K., Rasool, S., Glabe, C., Hock, C., and Nitsch, R. M. (2012) Early accumulation of intracellular fibrillar oligomers and late congophilic amyloid angiopathy in mice expressing the Osaka intra-Aβ APP mutation. *Transl. Psychiatry* **2**, e183
103. Soejima, N., Ohyagi, Y., Nakamura, N., Himeno, E., M. Iinuma, K., Sakae, N., Yamasaki, R., Tabira, T., Murakami, K., Irie, K., Kinoshita, N., M. LaFerla, F., Kiyohara, Y., Iwaki, T., and Kira, J. (2013) Intracellular accumulation of toxic turn amyloid-β is associated with endoplasmic reticulum stress in Alzheimer's disease. *Curr. Alzheimer Res.* **10**, 11-20
104. Sinha, S., Lopes, D. H. J., and Bitan, G. (2012) A key role for lysine residues in amyloid β-protein folding, assembly, and toxicity. *ACS Chem. Neurosci.* **3**, 473-481
105. Petkova, A. T., Ishii, Y., Balbach, J. J., Antzutkin, O. N., Leapman, R. D., Delaglio, F., and Tycko, R. (2002) A structural model for Alzheimer's β-amyloid fibrils based on experimental constraints from solid state NMR. *Proc. Natl. Acad. Sci. USA* **99**, 16742-16747
106. LeVine, H., Lampe, L., Abdelmoti, L., and Augelli-Szafran, C. E. (2012) Dihydroxybenzoic acid isomers differentially dissociate soluble biotinyl-Aβ(1–42) oligomers. *Biochemistry* **51**, 307-315
107. Abelein, A., Bolognesi, B., Dobson, C. M., Gräslund, A., and Lendel, C.

(2012) Hydrophobicity and conformational change as mechanistic determinants for nonspecific modulators of amyloid β self-assembly. *Biochemistry* **51**, 126-137

108. Huong, V. T., Shimanouchi, T., Shimauchi, N., Yagi, H., Umakoshi, H., Goto, Y., and Kuboi, R. (2010) Catechol derivatives inhibit the fibril formation of amyloid-β peptides. *J. Biosci. Bioeng.* **109**, 629-634
109. Palhano, F. L., Lee, J., Grimster, N. P., and Kelly, J. W. (2013) Toward the molecular mechanism(s) by which EGCG treatment remodels mature amyloid fibrils. *J. Am. Chem. Soc.* **135**, 7503-7510
110. Booth, A. N., and Deeds, F. (1958) The toxicity and metabolism of dihydroquercetin. *J. Am. Pharm. Assoc.* **47**, 183-184
111. Pozharitskaya, O. N., Karlina, M. V., Shikov, A. N., Kosman, V. M., Makarova, M. N., and Makarov, V. G. (2009) Determination and pharmacokinetic study of taxifolin in rabbit plasma by high-performance liquid chromatography. *Phytomedicine* **16**, 244-251
112. de Boer, V. C., Dihal, A. A., van der Woude, H., Arts, I. C., Wolffram, S., Alink, G. M., Rietjens, I. M., Keijer, J., and Hollman, P. C. (2005) Tissue distribution of quercetin in rats and pigs. *J. Nutr.* **135**, 1718-1725
113. Youdim, K. A., Qaiser, M. Z., Begley, D. J., Rice-Evans, C. A., and Abbott, N. J. (2004) Flavonoid permeability across an in situ model of the blood–brain barrier. *Free Radic. Biol. Med.* **36**, 592-604
114. Yang, F., Lim, G. P., Begum, A. N., Ubeda, O. J., Simmons, M. R., Ambegaokar, S. S., Chen, P. P., Kayed, R., Glabe, C. G., Frautschy, S. A., and Cole, G. M. (2005) Curcumin inhibits formation of amyloid β oligomers and fibrils, binds plaques, and reduces amyloid *in vivo*. *J. Biol. Chem.* **280**, 5892-5901
115. Jeon, S., Chun, W., Choi, Y., and Kwon, Y. (2008) Cytotoxic constituents from the bark of *Salix hulteni*. *Arch. Pharm. Res.* **31**, 978-982
116. Kuroyanagi, M., Yamamoto, Y., Fukushima, S., Ueno, A., Noro, T., and Miyase, T. (1982) Chemical studies on the constituents of *Polygonum nodosum*. *Chem. Pharm. Bull.* **30**, 1602-1608
117. Takegoshi, K., Nakamura, S., and Terao, T. (2003) $^{13}C$– $^{1}H$ dipolar-driven $^{13}C$–$^{13}C$ recoupling without $^{13}C$ rf irradiation in nuclear magnetic resonance of rotating solids. *J. Chem. Phys.* **118**, 2325-2341
118. Takegoshi, K., Nakamura, S., and Terao, T. (2001) $^{13}C$–$^{1}H$ dipolar-assisted rotational resonance in magic-angle spinning NMR. *Chem. Phys. Lett.* **344**, 631-637
119. Fields, C. G., Fields, G. B., Noble, R. L., and Cross, T. A. (1989) Solid phase peptide synthesis of $^{15}N$-gramicidins A, B, and C and high performance liquid chromatographic purification. *Int. J. Pept. Protein Res.* **33**, 298-303
120. Wiejak, S., Masiukiewicz, E., and Rzeszotarska, B. (1999) A large scale synthesis of mono- and di-urethane derivatives of lysine. *Chem. Pharm. Bull.* **47**, 1489-1490
121. Markham, K. R., and Ternai, B. (1976) $^{13}C$ NMR of flavonoids—II :

flavonoids other then flavone and flavonol aglycones. *Tetrahedron* **32**, 2607-2612

122. Bruschweiler, R. (2004) Theory of covariance nuclear magnetic resonance spectroscopy. *J. Chem. Phys.* **121**, 409-414

123. Trbovic, N., Smirnov, S., Zhang, F., and Brüschweiler, R. (2004) Covariance NMR spectroscopy by singular value decomposition. *J. Magn. Res.* **171**, 277-283

# List of publications

## 1. Original Papers

1) Mizuho Sato, Kazuma Murakami, Mayumi Uno, Haruko Ikubo, Yu Nakagawa, Sumie Katayama, Ken-ichi Akagi and Kazuhiro Irie (2013) Structure-activity relationship for (+)-taxifolin isolated from silymarin as an inhibitor of amyloid β aggregation.
*Biosci. Biotechnol. Biochem.*, **77**, 1100-1103.

2) Mizuho Sato, Kazuma Murakami, Mayumi Uno, Yu Nakagawa, Sumie Katayama, Ken-ichi Akagi, Yuichi Masuda, Kiyonori Takegoshi and Kazuhiro Irie (2013) Site-specific inhibitory mechanisms for amyloid-β42 aggregation by catechol-type flavonoids targeting the Lys residues.
*J. Biol. Chem.*, **288**, 23212-23224.

## 2. Related Papers

1) Naotaka Izuo, Toshiaki Kume, Mizuho Sato, Kazuma Murakami, Kazuhiro Irie, Yasuhiko Izumi, and Akinori Akaike (2012) Toxicity in rat primary neurons through the cellular oxidative stress induced by the turn formation at positions 22 and 23 of Aβ42.
*ACS Chem. Neurosci.*, **3**, 674-681.

2) Naotaka Izuo, Kazuma Murakami, Mizuho Sato, Mami Iwasaki, Yasuhiko Izumi, Takahiko Shimizu, Akinori Akaike, Kazuhiro Irie, and Toshiaki Kume (2013) Non-toxic conformer of amyloid β may suppress amyloid β-induced toxicity in rat primary neurons: Implications for a novel therapeutic strategy for Alzheimer's disease.
*Biochem. Biophys. Res. Commun.*, **438**, 1-5.